Characterization of Envelopes Thermal Transmittance based on a mixed approach

Auteur : Rifà Álamo, Roger
Promoteur(s) : Attia, Shady
Faculté : Faculté des Sciences appliquées
Diplôme : Cours supplémentaires destinés aux étudiants d'échange (Erasmus, ...)
Année académique : 2021-2022
URI/URL : http://hdl.handle.net/2268.2/13931

University of Liège

Faculty of Applied Science

—

Characterization of envelopes thermal transmittance based on a mixed approach

Master's thesis in order to obtain a master degree in
Industrial Engineering,
by **RIFÀ ÁLAMO Roger**

Supervisor: Prof. ATTIA Shady - SBD Lab
Jury: Dr. AMARIPADATH Deepak
Dr. DUBOIS Samuel

Academic year 2021-2022

Thesis Abstract

In Wallonia, there are many buildings and houses built in the 1960s, after World War II, that have envelopes and facades with many heat losses. Due to the poverty of the envelopes of these buildings, they are very energetically inefficient buildings (Attia et al., 2021) that need to be overheated in cold seasons to be comfortable inside.

For this matter, it has been developed a methodology through infrared thermography in order to detect the poorest elements of the envelopes of these buildings for a possible renovation. This study takes as a reference a building of the University of Liege residence built in 1968. The first stage of the work consists of making a 3D model of the building. This model has been made from images obtained by drone and printing it with a 3D printer to evaluate the accuracy of the method. The second part of the work consists of estimating the thermal transmittance (U-value) of the facade of the residence through infrared thermography. This method will be compared with real monitoring of the U-value using measurement sensors and the calculation of the U-value following the ISO 9869 standard. The study aims to compare the three methods in terms of accuracy, speed, usability, and cost.

The main results of this study have been to obtain the U-value by the three developed methods and the detailed comparison of these. A 3D modelling method has also been developed through images captured with the drone where good accuracy is achieved.

This study provides an interesting basis for future research using drones equipped with thermal cameras to develop 3D thermal models of buildings.

Keywords

Thermal transmittance (U-value), 3D modelling, 3D printing, Infrared thermography (IRT), Unmanned Aerial Vehicles (UAV).

Thesis Summary

Characterization of envelopes thermal transmittance based on a mixed approach

In the region of Wallonia, there are a large number of buildings constructed in the 1960s, after World War II. These buildings have significant heat losses in their envelopes and facades. This problem causes a significant increase in the energy consumption of these buildings, which is becoming an unsustainable situation for the environment.

This study proposes a method of identifying the thermal losses of building envelopes by focusing on the estimation or calculation of the thermal transmittance (U-value) of building facades. The three methods used are thermal image estimation with a hand-held camera, real-time monitoring using heat flux sensors and U-value calculations according to the ISO 9869 standard.

In addition, this work elaborates a methodology to estimate heat losses in a fast and efficient way employing aerial thermography using Unmanned Aerial Vehicles (UAV). As a UAV equipped with a thermal camera is not available, a methodology is developed using a drone with a normal camera that uses images of the building of the residence of the University of Liège to elaborate a 3D model in order to print it on a 3D printer and evaluate the accuracy of the method and to serve as a basis for future research into 3D thermal modelling of buildings.

In the methodology section, the three methods of calculation or estimation of the thermal transmittance of the building walls are described in detail. Also, a 19-step methodology is developed on how to obtain a 3D printing of the building from images captured with the drone.

The results obtained for thermal transmittance show that the most accurate method is real-time monitoring. A fairly good estimation is achieved by thermal imaging, which is close to the value of the monitoring estimation. As far as the calculations according to ISO 9869 standards are concerned, they are far from reality and confirm the degradation of the insulation of the building walls. With the results obtained, a comparison of the three methods is made in terms of accuracy, speed, cost and usability.

Following the elaborate methodology of 3D modelling from images of the Dorne, a 3D printing with good accuracy is achieved, which serves to validate the elaborate method.

Finally, the results obtained are discussed and the research questions raised are answered. The strengths and limitations of the work carried out are also presented, and finally, future research work is defined.

Acknowledgments

This thesis has become a reality with the kind support of many people. I would like to express my sincere thanks to each one of them.

First, I would like to express my deep gratitude to my supervisor Prof. Shady Attia, for accepting me into his laboratory and allowing me to work with him. Thanks to his valuable advice, constant supervision and motivation during the research, I have been able to learn a lot in fields unknown to me and to complete this thesis.

I would like to acknowledge the Sustainable Building Design Lab and all its members for monitoring equipment in this research, for guiding me throughout this research and for their valuable feedback and support.

I am especially thankful to Mr Mathieu Trofs and Mr Antoine Desiron from the A&M Department of ULiege to help me in the 3D printing process.

I would also like to thank Dr Samuel Dubois for hosting us in his offices at the Belgian Building Research Institute (BBRI) and guiding me on the methodology of the 3D modelling of the building.

Finally, I would like to thank my family, Berta and my Erasmus friends for supporting me, for believing in me to do this work in a foreign country with a foreign language and for accompanying me in this enriching Erasmus adventure.

Abbreviations/Acronyms

ASTM	American Society for Testing and Materials
BBRI	Belgian Building Research Institute
GHG	Green House Gas
IPCC	Intergovernmental Panel on Climate Change
IRT	Infrared thermography
ISO	International Organization for Standardization
NDT	Non-destructive testing
SBD Lab	Sustainable Building Design Laboratory
TI	Thermal image
UAV	Unmanned Aerial Vehicles
U-value	Thermal transmittance
3D	Three-dimensional

Table of Contents

List of Figures

List of Tables

1 Introduction

A very important part of a building is its façade and envelope. The envelope of a building is not only an outer layer, it is the first impact on energy performance. The thermal energy consumption of a building goes hand in hand with its external insulation. For this reason, correct identification of heat losses in building envelopes can allow us to locate serious anomalies in building and identify the elements that need future renovation.

Nowadays several tools can be very useful to analyse building envelopes, such as Unmanned Aerial Vehicle (UAV) in combination with infrared thermography. In this study, we will see how these tools can allow us to quickly assess the envelope of a building and detect anomalies (Rakha et al., 2021).

1.1 Background information and problem statement

In Wallonia, there are many houses built in the 1960s post-World War II that are very energy inefficient as they have a lot of heat loss in their envelopes and facades. Suburbanisation after World War II allowed many dwellers to live in single-family houses. As a result, the volume of property owners increased and houses were built without meeting any energy efficiency requirements and were built inefficiently. Today, a large number of these dwellings are occupied by elderly retired people. In Belgium, post-World War II households account for 48% of the existing building stock. (Attia et al., 2021).

This study aims to investigate a method of detecting façade anomalies or heat loss that can be used to detect the thermal inefficiencies of this large volume of outdated buildings.

A building built at that time has been selected for analysis and to test the methods to be developed. The study area of this work is a building of the University of Liege, specifically the Building 13 - Résidence Universitaire de l'ULiège located in Chem. du Trèfle, 4000 Liège. This building, built-in 1968, has many energy deficiencies that result in significant thermal losses due to the low thermal tightness of its enclosures and envelopes. The building consists of three identical towers as can be seen in Figure 1-1, however, the study will focus on the tower located to the southeast, which is the closest in the picture.

The construction materials of the facades of this building are reinforced concrete and a thin layer of rock wool insulation. The hypothesis developed is that the building envelope is in very bad condition and the degradation of the insulation suffered over the years makes its function almost null and void. In this study, we will try to validate this hypothesis.

Figure 1-1: Building 13 - Résidence universitaire de l'ULiège.

1.2 Relevance of the research topic

This study aims to investigate a fast and efficient method of calculating the thermal transmittance (U-value) of a building. Therefore, the main objective of the work is to estimate the U-value employing infrared thermography. This estimation process is intended to be relevant in order to detect important thermal gaps due to degradation of building façade components and to identify needs for future renovation. This estimate will be compared with more popular methods such as real-time monitoring using heat flux sensors and with the calculation according to the appropriate standards.

On the other hand, another objective of the work is to elaborate a methodology to create a 3D model of the building from thermal images obtained by a drone. This methodology is intended to be the first basis for future research projects to be developed at the Sustainable Building Design Laboratory of the University of Liege. Unfortunately, as a drone equipped with a thermal camera was not available, we will try to elaborate a 3D model of the building using a drone with a normal camera and evaluate the accuracy of the method by printing this model on a 3D printer. In any case, thermal images will be taken with a hand-held camera to estimate the U-value of the building walls and look for possible anomalies.

The stakeholders for whom this work is intended, i.e. the main audience that can benefit from our findings, are listed below:

- Skywin (aerospace cluster of Wallonia).
- Belgian Building Research Institute (BBRI).
- Belgian Civil Drone Council.

- Energy efficiency building auditors.

- Construction engineers, architectural engineers, architects, and researchers in these fields.

To make the relevance of this study more concrete, the main innovation and impact of this research study are summarised below:

- The innovation of this project is to elaborate the methodology to obtain a 3D model and a maquette of the building through the images obtained from a drone.

- Achieve a methodology for fast detection of the most important deficiencies in the facade of a building through thermal imaging. This methodology can be more effective in terms of cost, speed, and it could be an interesting fact of being able to measure it without having to enter the building (Rakha et al., 2021).

- A comparison of the three methods used to obtain the thermal transmittance of the building envelopes, which are real monitoring of the U-value, calculation method following the standard ISO 9869, and U-value estimations based on thermal imaging, in terms of accuracy, speed, cost, and usability.

1.3 Research Objectives

In this section, the objectives of this study are set out, followed by the definition of the research questions.

The objectives of this work are:

- Make a virtual 3D model of the building using pictures obtained with the drone and the Agisoft Metashape software.

- Convert the 3D model of the building to a vector printable version and print the model with a 3D printer.

- Using thermal images, estimate the values of thermal transmittance (U-value) of the building envelope.

- Evaluate data by real monitoring of the U-value with the heat flux sensor and the calculation method following the standard ISO 9869.

In order to achieve these objectives, we have set out three research questions:

- How to get a 3D model and a 3D printed maquette of a building through pictures obtained from a drone?

- How to estimate the values of thermal transmittance (U-value) of a building envelope using thermal images?

- How do the U-values obtained from (i) real monitoring using heat flow sensors, (ii) calculation method according to the standard ISO 9869, and (iii) estimations based on thermal imaging differ in terms of accuracy, speed, cost, and usability?

1.4 Quad Chard

To synthesise and group all the information presented in the introduction, we have created a Quad Chard shown in Figure 1-2.

Characterization of Envelopes Thermal Transmittance based on a mixed approach

Aims/Objective	Audience or Stakeholders
• Make a virtual 3D model of the building using pictures obtained with the drone and the *Agisoft Metashape* software. • Convert the 3D model of the building to a vector printable version and print the model with a 3D printer. • Using thermal images, estimate the values of thermal transmittance (U-value) of the building envelope. • Evaluate data by a real monitoring and the calculation method following the standard ISO 9869.	• Skywin (aerospace cluster of Wallonia). • Belgian Building Research Institute (BBRI) Dr. Dubois. • Belgian Civil Drone Council. • Energy efficiency building auditors. • Construction engineers, architectural engineers, architects and researchers in these fields.
Innovation	**Impact**
• Elaborate the methodology to obtain a 3D model and a maquette of the building through the images obtained from a drone. • The proposed methodology can be very useful in order to analyze the deficiencies or problems of buildings envelopes. • A comparison of the three methods used to obtain the thermal transmittance of the building envelopes.	• The 3D modeling method can serve as a basis for the next step which would be a thermal model using thermal drones. • Quickly and accurately identify the most energetically critical areas of building facades for future renovation without the need to enter the building. • Classification of the methods used in terms of accuracy, speed, cost and usability.

Figure 1-2: Quad Chard.

Finally, we present the expected outcomes we want to achieve:

- Virtual 3D model of the building.

- 3D printing of the building.

- Thermal images captured by a hand-held thermal camera.

- Estimation of thermal transmittance(U-value) of the building envelope.

- Comparison of (i) real monitoring using heat flow sensors, (ii) calculation method according to the standard ISO 9869, and (iii) estimations based on thermal imaging differ in terms of accuracy, speed, cost, and usability.

2 Literature review

This is the chapter where the theoretical basis of the main topics discussed throughout the thesis is presented. This chapter is composed of the sections: state of the art of the theories & concepts of the study, concepts and variables of your research, similar studies and Knowledge gap.

2.1 State of the art of the theories & concepts of the study

In this section, we will deal with the main topics one by one in a theoretical way. We will start with the background of the study, then we will deal with infrared thermography, aerial thermography and the operation of the 3D image modelling software that we will use (Agisoft Metashape).

2.1.1 Background information

Climate change and energy consumption are two of the most critical matters that humanity will confront over the next two decades. Energy efficiency is regarded as one of the major impediments to proceeding toward the global goal of reducing Green House Gas emissions (GHG) (Attia et al., 2021). Built environments make a significant contribution to climate change mitigation. However, existing buildings, which comprise the majority of urban infrastructures, do not usually meet today's rigorous energy efficiency standards (IPCC, 2014). As they naturally deteriorate over time, they adversely contribute to their surrounding environments. Accordingly, frameworks and approaches for accurate Building Energy Model (BEM) simulations are required to enhance retrofitting design solutions that could deliver existing buildings fairly close to current efficiency standards.

Optimizing the thermal efficiency of the existing building stock is vital for reducing the overall energy consumption in the building sector. The evaluation of the building envelope's actual thermal performance is a prerequisite in the optimization process. Commercial energy consumption can be reduced by 57% and residential energy consumption can be reduced by 42% with improvements in building envelopes (Bayomi et al., 2021). Thermal transmittance (U- value) represents the amount of heat transfer of the building envelope, which is one of the key factors that is necessarily tied to the thermal performance of the envelope (International Energy Agency (IEA), 2014). The envelope U-value, on the other hand, is not constant because it is strongly impacted over time by surrounding climatic conditions, the level of post-occupancy maintenance, and the material condition of the façade (IPCC, 2014).

Among the readily accessible non-destructive testing (NDT) techniques, infrared thermography (IRT) is now widely used for building diagnostics. IRT is based on measuring the radiant thermal energy distribution emitted by a target (O'Grady, M. et al., 2017). IRT approaches for qualitative and quantitative assessments of building diagnostics range from passive to active. Nevertheless, several factors affect the accuracy of the assessment, even though IRT is a useful tool for evaluating envelope performance (Kylili, A. et al., 2014). Its effectiveness stems from the ability to capture high-resolution data with significant time efficiency and minimal reliance on human labour (Rakha et al., 2018).

For building and site audits, there are typically three levels of audit (Thumann, P.E., et al., 2017):

- Walkthrough: Building energy system data are analyzed and quantified through a visual inspection to determine average energy consumption and set benchmarks.

- Energy Audit: This presents a systematic analysis of building energy losses and the characteristics of energy systems based on on-site measurements. Moreover, the effectiveness of building systems and energy conservation measures are also investigated at this level.

- Investment Grade: In order to predict annual energy consumption, energy simulation models are developed and used. considering weather conditions, building systems, and occupancy schedules.

2.1.2 Infrared thermography

To investigate thermal anomalies, two approaches are used: qualitative and quantitative IRT (Schwoegler, M., 2006). Between the two methodologies, there is a variation in how measurements are conducted. Quantitative IRT relies on numerical analysis to identify and quantify thermal anomalies (Pearson, C., 2011). Whereas qualitative IRT is used to determine the presence of thermal anomalies through visual assessment of temperature variations in the observed radiation spectrum. It should be emphasized that qualitative measurements only differentiate probable thermal anomalies, and they are not to determine the degree of deficiencies. Accordingly, this method is utilized primarily when thermal anomalies may be easily detected (Fox, M. et al., 2014). Qualitative thermography is widely used to detect thermal anomalies induced by high thermal transmittance. Thermal bridges, on the other hand, are typically found using quantitative thermography (Francesco, A. et al., 2011).

2.1.3 Aerial thermography

Advances in inspection using UAVs have enabled professionals to have a very interesting tool to examine building envelopes accurately and quickly with minimal cost and safe risk (Bayomi et al., 2021; Rakha et al., 2021). The use of aerial thermography opens a new window for auditors as it provides them with interesting information for their reports (Mauriello, M.L. et al., 2015).

All these advantages have to take into account that specific conditions must be met in order to obtain valid results. First, some environmental conditions have to be avoided during UAV flights, such as rain, snow and strong wind. Secondly, other weather phenomena can detract from the results obtained by thermography. It is advisable to avoid recording data on surfaces exposed to sunlight, solar loading and self-shading, as these can significantly affect thermal imaging outcomes. It is advisable to capture RGB images at the same time as the thermal images to clarify the conditions at the time of inspection. Third, external surface temperatures can be affected by high ambient humidity, wind speed and precipitation. It is therefore recommended not to collect data in these critical situations (Bayomi et al., 2021).

Another limitation of airborne thermography is that in order to estimate the thermal transmittance, additional data is needed to those obtained using UAVs. Detailed information is required on the building construction materials and their thermal properties, as well as the thermal conditions inside the building.

Finally, when capturing reflected light on shiny surfaces such as glass and metal, we cannot rely on the thermal readings, as they will not be true. To avoid reflection problems, it is recommended to capture thermal images perpendicular to the surface being analysed at an appropriate distance (Bayomi et al., 2021).

When using UAVs in conjunction with IR imaging, there are three major procedures that must be meticulously planned (Rakha, T. & Gorodetsky, A., 2018):

1) Site Acquisition, which includes individual building audits, surveying of building clusters, and planning for data obscuring through obstacles such as trees, street furniture, etc.

2) Flight Path Planning, which includes identifying survey locations (interiors and exteriors), the audit focus, and envelope components such as windows and doors, as well as flight path design considerations such as distances from targets, bearing angles, and drone altitudes.

3) Post-flight data analysis techniques, such as data formatting, quantitative and quantitative methods, and image processing techniques, with potential 3D photogrammetry integration.

2.1.4 Agisoft Metashape algorithm

The software used to convert images of the building into a 3D model of the building is Agisoft Metashape. This interesting process can be done thanks to a procedure used by the software described below ().

- Feature matching across the photos. Detection of stable points that later serve to detect correspondences between the photos.

- Solving for camera intrinsic and extrinsic orientation parameters. A greedy algorithm is used to find approximate camera locations and refine them later using a bundle-adjustment algorithm.

- Dense surface reconstruction. Several processing algorithms are available. Smooth and Height-field methods are based on pair-wise depth map computation, while fast method utilizes a multi-view approach.

- Texture mapping. Parametrizes of surface possibly cutting it into smaller pieces and then blends source photos to form a texture atlas.

2.2 Similar studies

In this study, we have mainly used two similar studies as a reference.

The first study is from (Bayomi et al., 2021), an article in the scientific journal Energy & Buildings 2021 entitled "*Building envelope modelling calibration using aerial thermography*". This paper describes research that focuses explicitly on calibrating

envelopes of existing BEMs with thermography sensors using drones. The research focuses on the automation of on-the-fly envelope U-value estimations as well as the verification of calibrated envelope BEMs. The paper uses thermal imagine representing material degradation, thermal bridging, and insulation failures in a renovated campus building in Boston, MA. Following that, a BEM is calibrated, and post-renovation metered and modeled wintertime heating energy are compared. The goodness of fit measures shows an improvement in BEM performance from 21.8% to 0.9%, demonstrating the utility of the proposed framework.

The second study is by (Rakha et al., 2021), and its title is "*3D Drone-based Time-lapse Thermography: A Case Study of Roof Vulnerability Characterization using Photogrammetry and Performance Simulation Implications*". This paper presents a novel workflow for 3D envelope modeling based on aerial timelapse IR data collected using Unmanned Aerial Systems (UAS). Using photogrammetry software Agisoft Photoscan, which generates temporal IR inspections of building skins using multiple 3D thermography CAD models, a comprehensive envelope thermal profile is created for the roof of a case study building. The ultimate goal is to create a framework for building inspections that use UAS equipped with IR cameras to collect data time series, which then informs envelope modeling for accurate performance simulation.

3 Methodology

This chapter describes the methodology applied in order to answer the research questions. The research questions presented in the first chapter are:

- How to get a 3D model and a 3D printed maquette of a building through pictures obtained from a drone?

- How to estimate the values of thermal transmittance (U-value) of a building envelope using thermal images?

- How do the U-values obtained from (i) real monitoring using heat flow sensors, (ii) calculation method according to the standard ISO 9869, and (iii) estimations based on thermal imaging differ in terms of accuracy, speed, cost, and usability?

To answer these questions, we first explain in detail the process to get a 3D print starting as a basis with the images obtained by a drone. Next, the methodology is followed by the three methods of calculating the thermal transmittance of the building and obtaining the U-value. Research design is defined by the four established steps which are data collection, data processing, instrument or methodology creation, and application validation.

3.1 Description of the research design and methods

To answer the first research question that is "How to get a 3D model and a 3D printed maquette of a building through pictures obtained from a drone?", the research design used is to create a method based on experimentation and exploration of different pathways and possibilities. This stage of the work corresponds to a validation of the creation of the 3D model through the recognition of images, which ends with the printing of a 3D model in order to validate the accuracy of the method.

The second research question posed is "How to estimate the values of thermal transmittance (U-value) of a building envelope using thermal images?". To answer this research question, we followed the procedure used in (Bayomi et al., 2021), which proposes a numerical approximation of the value of thermal transmittance from the surface and ambient temperatures of the research object. In this way, we have obtained an estimation of the U-value through the captured thermal images.

Finally, to answer the third research question about "How do the U-values obtained from (i) real monitoring using heat flow sensors, (ii) calculation method according to the standard ISO 9869, and (iii) estimations based on thermal imaging differ in terms of accuracy, speed, cost, and usability?", we describe the methodology used to obtain the other thermal transmittance results. The equipment used for the actual monitoring of the U-value is defined, as well as the conditions that must be met to achieve a correct result. The calculation method according to the ISO 9869 standard is also explained. Finally, we will compare the three methods in the following chapters.

3.2 Conceptual study framework

A conceptual framework of the study has been elaborated which summarizes in a graphical way the approach of the research and the methodology used. It is represented in Figure 3-1.
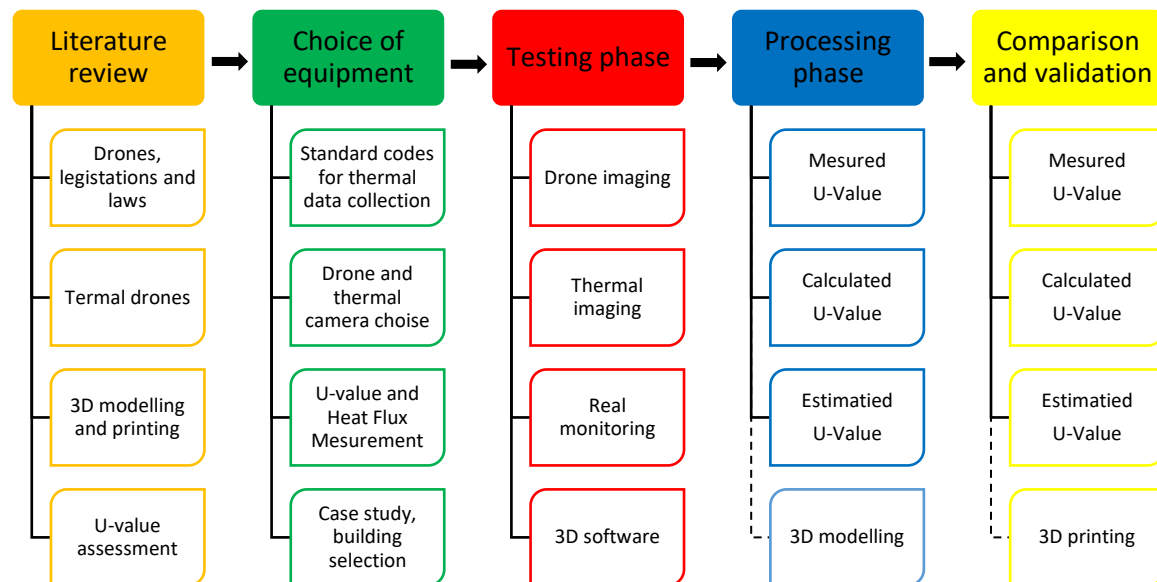
Figure 3-1: Conceptual study framework

The initial phase of this work consists of a literature review. We have researched publications and studies on the topic of the thesis in order to know that it has already been published and to acquire basic knowledge. In this way, drone models, drone legislation and policies, thermal drones, 3D modeling, 3D printing, and u-value assessment are all being researched.

The following steps are the selection of equipment, the establishment of standards to be followed, and the definition of the case study. In this section, we looked into how to capture thermal images correctly while adhering to industry standards. We've also decided on the type and model of drone we'll use to create our 3D model, taking into account the laws of unmanned aerial vehicles. We have chosen the heat flow measurement equipment that will be used to calculate thermal transmittance in real-time monitoring, such as the infrared camera used. Finally, we have decided on the building that will be the subject of our investigation.

After deciding on the equipment to use, the next step has been to become acquainted with it and begin collecting data. During this phase, we worked with drone flights, capturing images of the building for 3D modeling, thermal imaging of the building, heat flow sensor installation, and 3D modeling software testing.

During the processing phase, we worked with the obtained data to determine the value of thermal transmittance using the three previously defined pathways: real-time monitoring, calculation following the standards, and estimation using thermal images. Another aspect of this phase has been the work on the 3D model of the building based

on the recognition of images obtained by the drone, where we worked on the model to get a 3D printable version and validate the method's accuracy.

Finally, in the final stage of the study, we examined the three results obtained from the thermal transmittance of the studied building's walls. We assessed and compared the outcomes in terms of accuracy, cost, usability, and speed. We also got 3D printing of the building, allowing us to test the effectiveness of the image recognition method.

3.3 Operationalization: variables, indicators

This section explains the operationalization of the study variables, the indicators, and the source of the data used.

We will explain our central variable of the thesis, the value of the thermal transmittance (U-value) of the envelopes of the building B13 of the university residence to be analyzed. This variable is shown in Table 3-1 below.

Table 3-1: Thermal transmittance (U-value)

Variable	Definition	Indicators	Source of data
Thermal transmittance (U-value)	Heat transfers through a solid object, which is located between two fluids (gas or liquid) with different temperatures. The variable is defined in units of $W / m^2 \cdot K$.	- Accuracy: valuation of how it approaches real value. - Speed: time to calculate it. - Cost: cost of material needed. - Usability: overall relationship of the quality of the measure.	- Real-time monitoring. - Estimation from thermal images. - Calculation according to the standards.

Using the indicators shown, the variable on which this work focuses will be evaluated and compared. As previously stated, the U-value will be obtained through three different methodologies.

3.4 Data collection

In terms of data collection, this chapter is divided into four sections: U-value real-time monitoring, U-value calculation according to regulations, U-value estimation using thermal images, and the 3D model of the building. In each section, we explain how the data was collected, what equipment was used, and whether it came from our own source or from the literature.

3.4.1 U-value real-time monitoring

In order to carry out real-time monitoring of the thermal transmittance of the walls of the building to be analyzed, we used the gSKIN® U-Value Kit heat flow sensors from the greenTEG brand. Figure 3-2 shows the equipment mentioned. Data-sheet in Annex 1.

Figure 3-2: gSKIN® U-Value KIT (source: https://www.greenteg.com/U-Value/)

This kit delivers reliable quantitative in-situ information about a building envelope. The measurement approach uses a heat flux sensor and two temperature sensors and it is standardized in ISO 9869.

The method of placing the sensors is very simple. The heat flow sensor and a temperature sensor must be installed on the wall to measure the U value and the other temperature sensor on the outside of the building, on the other side of the wall.

Figure 3-3 shows the installation of the sensors inside a room of building B13 of the university residence.
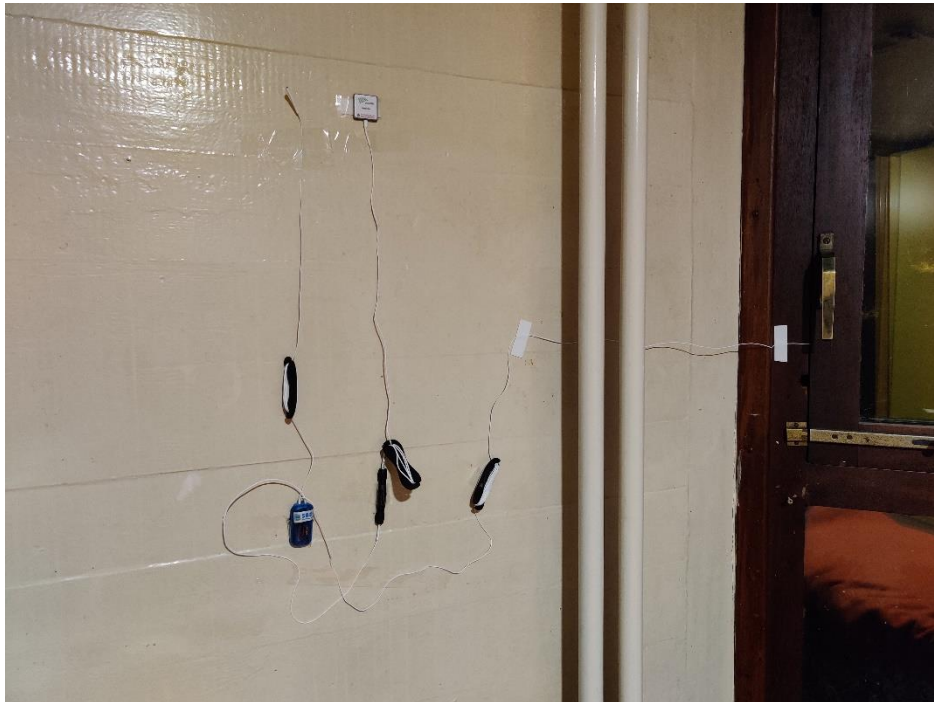
Figure 3-3: Heat flux sensor and temperature sensor installed inside the building.

Figure 3-4 and Figure 3-5 show the installation of the temperature sensor outside the building, on the other side of the wall where the inside sensors are installed.

Figure 3-4: External temperature sensor cable passage.

Figure 3-5: Temperature sensor installed outside the building.

To obtain a U-value approved according to the ISO 9869 standard, the following basic requirements must be met:

- A temperature difference of about 5ºC between inside and outside.

- Functional sensors.

- Measurement duration exceeding 72h.

- The last measured U-value differs less than 5% from U-value 24h before.

- No crossing of temperature curves (inside vs. outside).

In compliance with the requirements set out, the sensors were installed in a room on the ground floor of the B13 building in the south-east tower on November 23, 2021, at 7:00 pm.

Through the software provided by greenTEG, data were obtained every minute from the parameters listed in Table 3-2.

Table 3-2: Real monitoring variables.

Variable	Units
Heat Flux	W/m^2
T1 (internal temperature)	ºC
T2 (external temperature)	ºC
U-value	$W/m^2\,K$

3.4.2 U-value calculation following the standards

The ISO 9869-1:2014 standard was used to calculate the second approximation of the analyzed building's thermal transmittance value.

Regarding the collection of data in this process, it is necessary to know the dimensions and materials of the wall. For this reason, this information has been sought in relevant documentation in the report and plans of the building.

In Figure 3-6 and Figure 3-7 we can see a narrow cut of the plans of the building that shows the dimensions of the wall and its composition. The complete plan can be found in Annex 2.
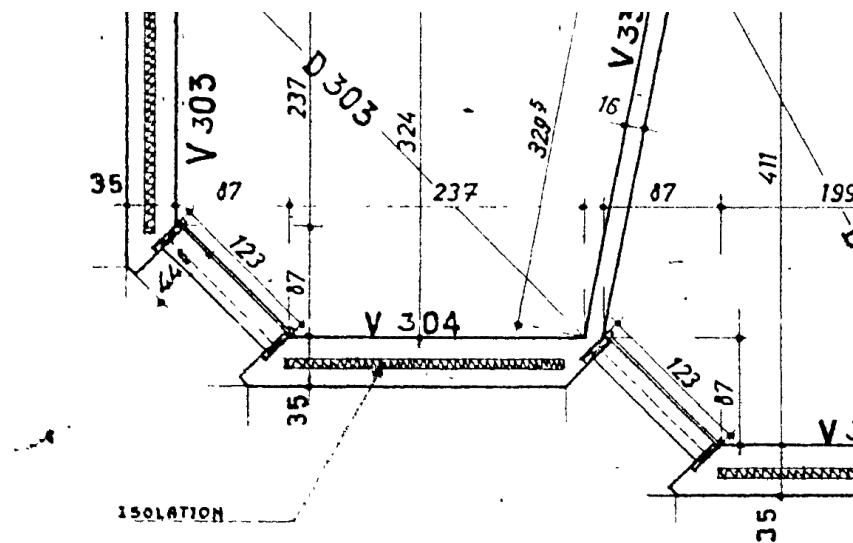
Figure 3-6: Capture of the building plan, wall composition.
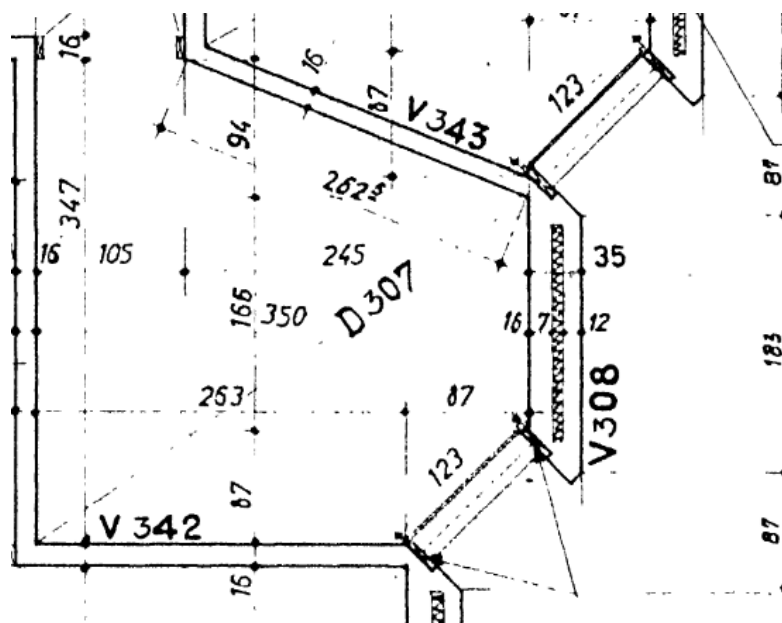
Figure 3-7: Capture of the building plan, wall dimensions.

As we can see in the plans the composition and dimensions of the wall from the inside to the outside are as follows:

- 16 cm of concrete.

- 7 cm of insulation rock wool (Heraclik).

- 12 cm of concrete.

The thermal conductivity values of the materials forming the walls of the building according to ISO 10456 are summarised in Table 3-3:

Table 3-3: Wall materials thermal conductivity.

Material	Thermal conductivity, λ [W/(m·K)]
Concrete (reinforced with 1% of steel)	2,3
Rock wool	0,035

3.4.3 U-value estimation from thermal imaging

The equipment used to estimate the U-value using infrared thermography (IRT) is a FLIR i7 hand-held thermal camera. This camera will allow us to obtain infrared images of the building envelope, to know the temperature of the building surfaces and to evaluate where the greatest thermal leakage occurs. Figure 3-8 shows a photograph of this camera. The technical data-sheet can be found in Annex 3.

Figure 3-8: FLIR i7 thermal camera (source: https://www.tequipment.net/fliri7.html)

The temperatures obtained with the thermal camera are:

- External wall surface temperature (T_s).
- Inner wall surface temperature ($T_{s,in}$).
- Reflection temperature (T_{refl}).

Figure 3-9 shows the actual and thermal images of how the temperature of the outer surface of the wall has been obtained.
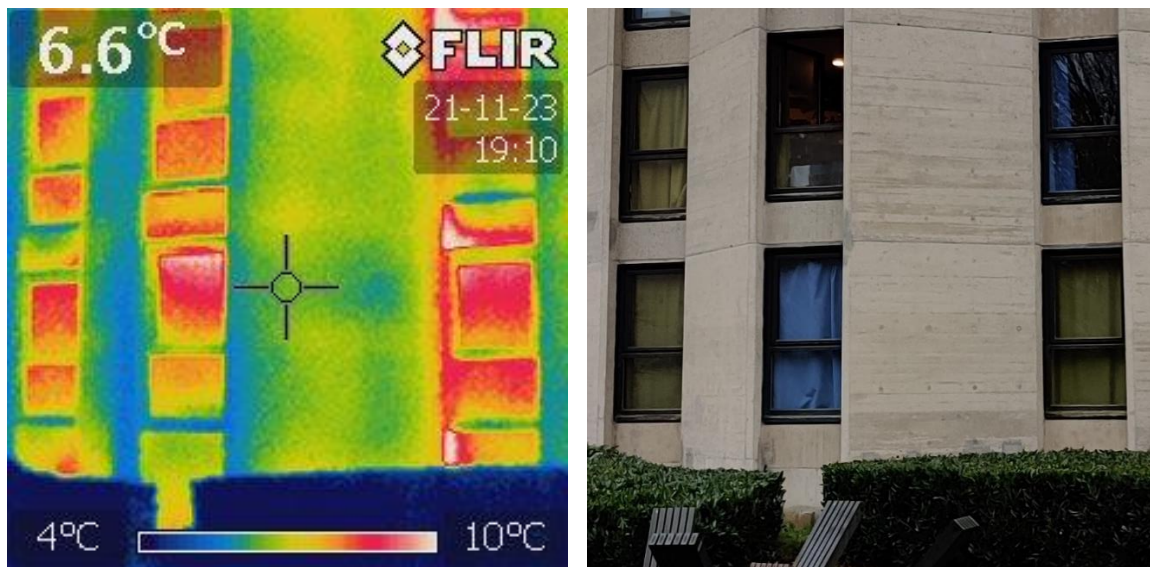
Figure 3-9: Thermal image and real image of the measuring point of the outer surface of the wall.

The reflection temperature was obtained following the procedure of (ASTM E1862-97, 1997), opting for the procedure using aluminium foil and setting the emissivity of the thermal camera to 1 ($\varepsilon = 1$).

As far as ambient temperatures are concerned, the values collected with the temperature sensors during the real-time monitoring are described in section 3.4.1.

Thermal images of different areas of the building envelope have also been captured to identify and locate possible irregular heat losses.

3.4.4 3D model of the building

As a drone with a thermal camera was not available, a normal drone was used. After analysing the market, the DJI Mini 2 model was chosen. This drone allows us to obtain the images of the building necessary to make the 3D model, and at the same time, it does not require a flight licence or a pilot's licence. This is thanks to its strategic weight of 249g, below the 250g limit set by the regulations.

Figure 3-10 shows the DJI mini 2 drone. Specifications can be found in Annex 4.

Figure 3-10: DJI Mini 2 (source:https://www.dji.com/be/mini-2)

Several drone flights were performed around the building in automatic flight modes, such as circular and spiral, centred on the target building. In each flight, the drone filmed the building from different angles and perspectives. Flights were also made in manual mode to film all the facades and the roof at close range. With these videos, we collected 270 images of the building from all points of view.

Figure 3-11 shows a sample of the photos collected. We have chosen to use a number of 270 images, as the number of images should not be excessive. The number of photos is optimal so that each photo must match those that overlap each other (Maharani et al., 2020). The number of photos that can be processed by Metashape depends on the available RAM and reconstruction parameters used (*Agisoft Metashape User Manual: Professional Edition, Version 1.8*, 2022). Another recommendation from the Agisoft Metashape manual on the number of photos is that it is better to have more photos than necessary than not enough.
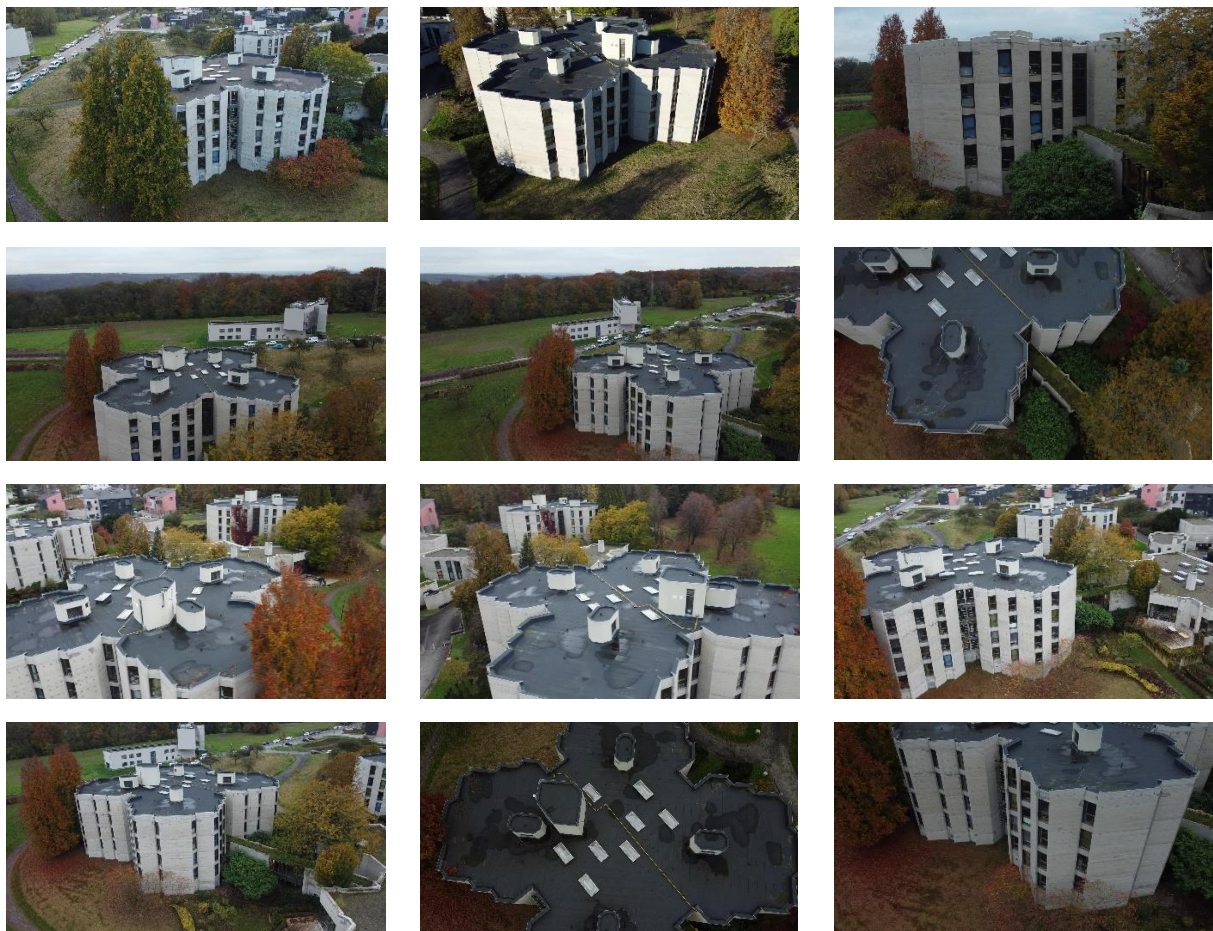

Figure 3-11: Sample of photos taken with the drone.

3.5 Data analysis

In this chapter, we will describe the data analysis and the process that has been carried out in each part of the work to achieve the results. In this way, the same sections as seen in the previous chapter 3.4 will be followed.

3.5.1 U-value real-time monitoring

After collecting monitoring data in accordance with all requirements imposed by the ISO 9869 standard, as explained in section 3.4.1, the data was downloaded in an excel spreadsheet to obtain the average values of the thermal transmittance of the building wall. In this way, we can represent a graph with the evolution of the curves of indoor temperature, outdoor temperature, heat flow, and U-value. In addition to the average U-value, the percentage of the variance of the U-value for the previous 24 hours has been calculated, as specified in the standard.

3.5.2 U-value calculation according to the standards

In this section, we explain the equations used to calculate the U-value following the ISO 9869-1:2014, Thermal insulation - Building elements – *In-Situ* measurement of thermal resistance and thermal transmittance (ISO 9869-1, 2014) and ISO 6946:2017, Building components and building elements – Thermal resistance and thermal transmittance – Calculation methods (ISO 6946, 2017).

The thermal transmittance of the element, represented by U [W/(m^2·K)]. U is given by (1).

$$U = \frac{q}{(T_i - T_e)} = \frac{1}{R_T} \tag{1}$$

where q [W/m^2] is the density of heat flow rate, T_i is the interior environmental temperature and, T_e is the exterior environmental temperature. We will use the second part of the equation where R_T is the total thermal resistance given by (2).

$$R_T = R_{si} + R + R_{se} \tag{2}$$

Where R_{si} and R_{se} are the internal and external surface thermal resistance, respectively.

We use Table 3-4 to find the values of R_{si} and R_{se} for a direction of the horizontal heat flow, extracted from ISO 6946.

Table 3-4: Conventional surface resistances.

Surface resistance [m²·K/W]	Direction of heat flow		
	Upwards	Horizontal	Downwards
R_{si}	0,10	0,13	0,17
R_{se}	0,04	0,04	0,04

R is the thermal resistance of an element [m²·K/W]. We will have to add the thermal resistances of all the layers that form the wall of the building. The thermal resistance of each layer, R_i, is computed using (3).

$$R_i = \frac{d_i}{\lambda_i} \tag{3}$$

Where:

d_i is the thickness of the layer [m];

λ_i is a thermal conductivity for the material of the layer [W/(m·K)], given in ISO 10456 shown in section 3.4.2 (Table 3-3).

Using the equations (1), (2) and, (3) we can obtain the calculated value of the thermal transmittance (U-value) of the walls of the analyzed building.

3.5.3 U-value estimation from thermal imaging

To estimate the U-value using infrared thermography, we relied primarily on the methodology by (Bayomi et al., 2021).

In the cited article, an equation (4) is developed that allows to estimate the thermal transmittance from surface temperatures obtained through the thermal images. This equation is a slight modification of the initial equation developed by (Madding, 2008).

The overall heat transfer coefficient is calculated using the following equation (4):

$$U = \frac{\varepsilon\sigma\left(T_{refl} - T_{s,in}\right) + h_c\left(T_{in} - T_{s,in}\right)}{T_{s,in} - T_{s,out}} \tag{4}$$

Where:

ε Emissivity

σ Stefan-Boltzmann constant   W·m⁻²·K⁻⁴

T_{refl} The apparent measured temperature   K

$T_{s,in}$ Interior wall surface temperature   K

$T_{s,out}$ External wall surface temperature   K

h_c	Convection Coefficient	W/(m²·K)
T_{in}	The indoor air temperature	K

To estimate the emissivity of the exterior wall, we followed (Bayomi et al., 2021) taking a value of 0,95.

A standardized convection coefficient (h_c) of 8,7 W/(m²·K) derived from (Tanner et al., 2011) was used to estimate U-value from IR data.

Regarding the temperatures required in the equation, we used a handheld camera as explained in section 3.4.3 of data collection.

To verify the dimensional consistency of the equation from (Bayomi et al., 2021):

$$U = \frac{W \cdot m^{-2} \cdot K^{-4} \cdot K^3 \cdot (K - K) + W \cdot m^{-2} \cdot K^{-1} \cdot K}{K - K}$$
$$= \frac{W \cdot m^{-2} \cdot K^{-4} \cdot K^4 + W \cdot m^{-2}}{K}$$
$$= \frac{W \cdot m^{-2} + W \cdot m^{-2}}{K}$$
$$= \frac{W}{m^2 \cdot K}$$

Apart from this quantitative estimation, we have also carried out a qualitative estimation by deeply analysing thermal images of the building envelopes as performed in (Bayomi et al., 2021). This analysis aims to identify irregular heat losses, based on the shape and the location of the anomaly, such as those described below:

- Thermal bridge: identification of vertical or horizontal anomalies of cladding located mainly around a corner of the building and between floors.

- Material degradation: degradation of cladding materials or cracks.

- Insulation failure: thermal leakage around doors and windows, and degradation of insulation in the building envelope.

We have used FLIR Thermal Studio software for the analysis of the thermal images (*FLIR Thermal Studio*, 2021).

These irregularities allow us to analyse qualitatively the thermal losses of the building.

3.5.4 3D model of the building

In this subsection we will explain the steps of the methodology to achieve a printable version of the building to be printed on a 3D printer, starting from the images collected with the UAV.

First of all, we present the software used in this study, including:

- Agisoft PhotoScan Professional 1.4.3: This software developed by Agisoft LLC performs the photogrammetric processing of digital images and generates 3D

spatial data (*Agisoft PhotoScan Professional 1.4.3*, 2022). It will allow us to generate a 3D model from images of the building.

- Meshmixer 3.5: It's a tool from Autodesk, Inc. is a prototype design tool based on high-resolution dynamic triangles meshes (*Meshmixer 3.5*, 2021). With this software, we will get a closed and solid model, suitable to be printed in 3D.

- PrusaSlicer 2.3.3: PrusaSlicer is an open-source, feature-rich, frequently updated tool that allows you to export the print files for Prusa 3D printer (*PrusaSlicer 2.3.3*, 2021). PrusaSlicer will allow us to slice our model and define the passes of the 3D printer.

- Pronterface: It is a 3D printing host software suite that talks to your printer and handles the printing process (*Pronterface*, 2021).

Secondly, we define the equipment used in this section, which consists of a high-performance workstation for image recognition simulation and the 3D printer used:

- The state of the art workstation at the SBD Lab, ULiège, uses a processor with 64 cores, 128 threads, and a 256MB cache for computing power and performance. This is in combination with 128GB (4 x 32GB) of memory (RAM) and a graphics card of 24GB.

    The main components are:

    - CPU: AMD Ryzen Threadripper 3990X, 64 x 2.9GHz, 256MB Cache, 280W TDP, TRX40.

    - RAM: 64GB – 2 x 32GB Kit DDR4-3200 CL16, Corsair Vengeance LPX (2 x 32 GB Kit x 2 St. = 128GB).

    - Graphics card: NVIDIA GeForce RTX 3090, 24GB.

    Figure 3-12 shows a photo of the used SBD lab workstation.
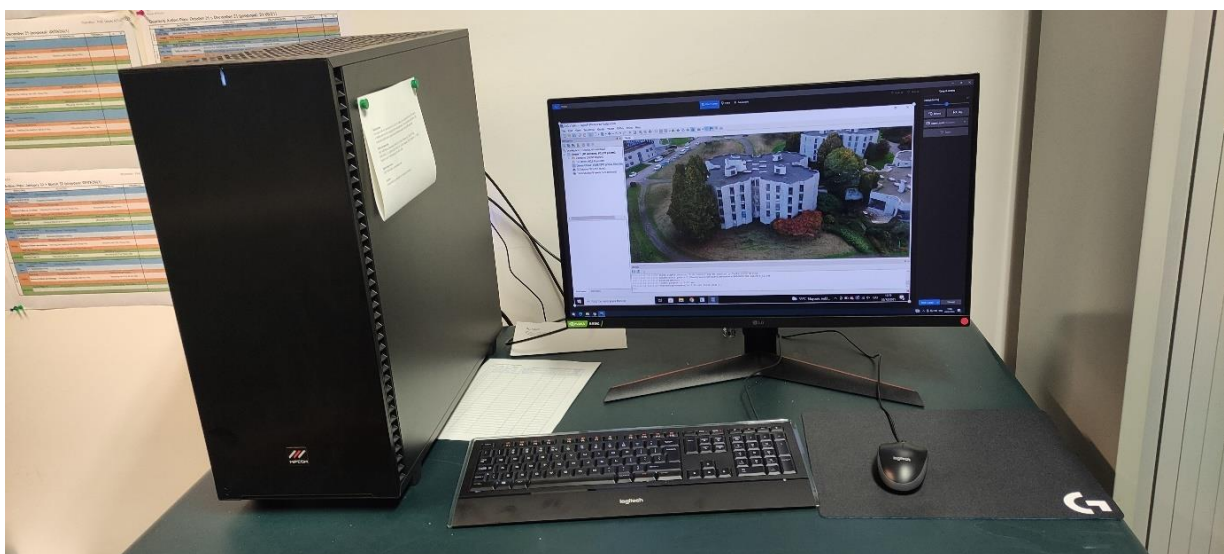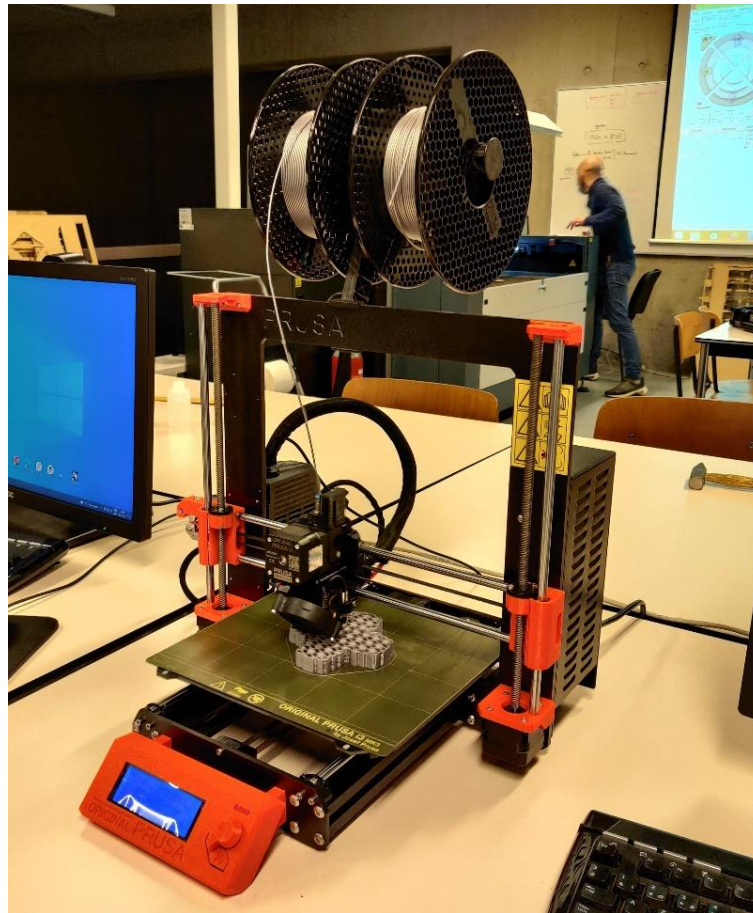

Figure 3-12: SBD Lab workstation.

- 3D printer: Original Prusa i3 MK3S (Figure 3-13). Data-sheet in Annex 5.

Figure 3-13: Original Prusa i3 MK3S.

Next, we will explain step by step the process followed, starting from the images of the building obtained with the drone to get a 3D printing:

1. The first programme we use is Agisoft Photoscan. To start our process we add the 270 photographs to the software. We can do this using the workflow menu. Then, the photos are aligned using the same menu and we select the low accuracy in the align settings. The software places all the pictures in the space with their correct position and tilt (Figure 3-14).
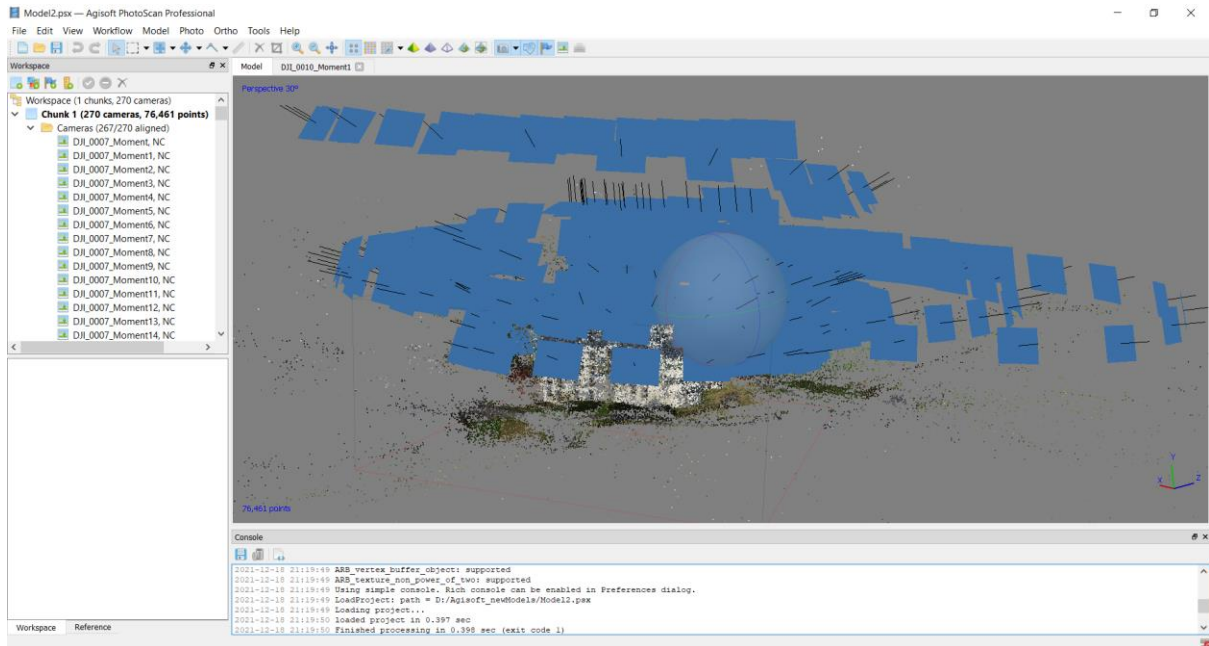

Figure 3-14: Agrisoft screenshot. Alignment of photographs in space.

At the same time, it creates a first point cloud of the 3D representation of the environment, where we can already start to recognise the building as we can see in Figure 3-15.
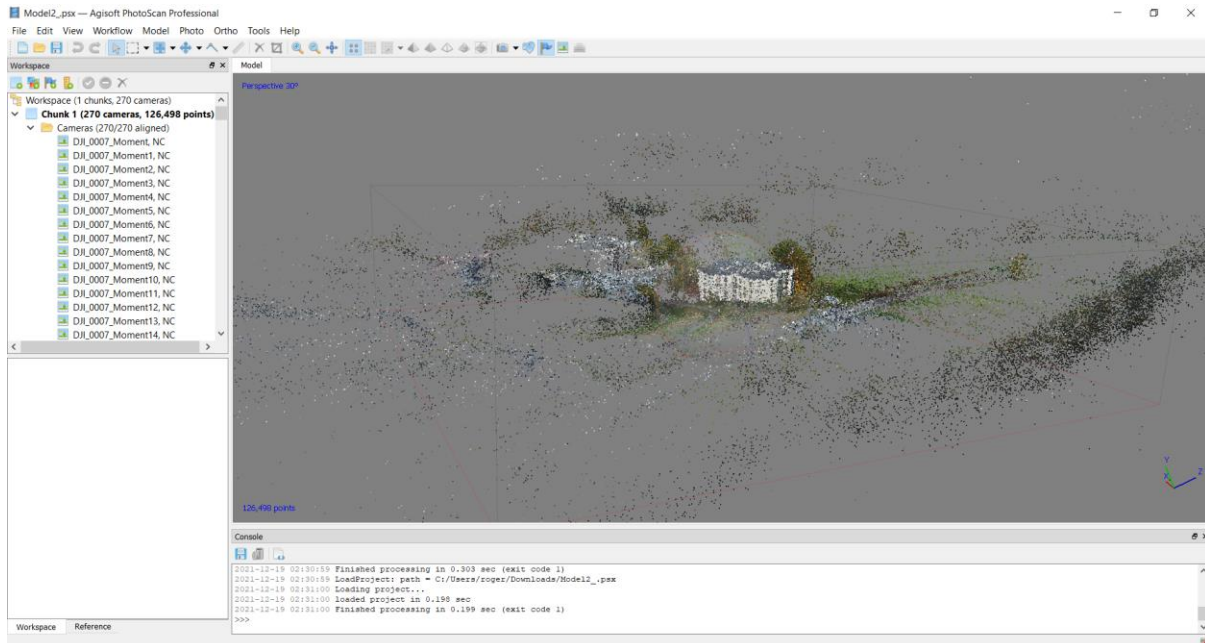
Figure 3-15: Agisoft screenshot. Point cloud.

2. In order not to lose details when the software comes to building the mesh and the texture of our building, we create some masks. We select two or three photographs from each flight and crop the building as shown in Figure 3-16. In this way, we eliminate information from around the building and the software will focus on defining the building's junction points. At the same time, it will not waste time and resources on modelling spaces outside the building that we are not interested in.
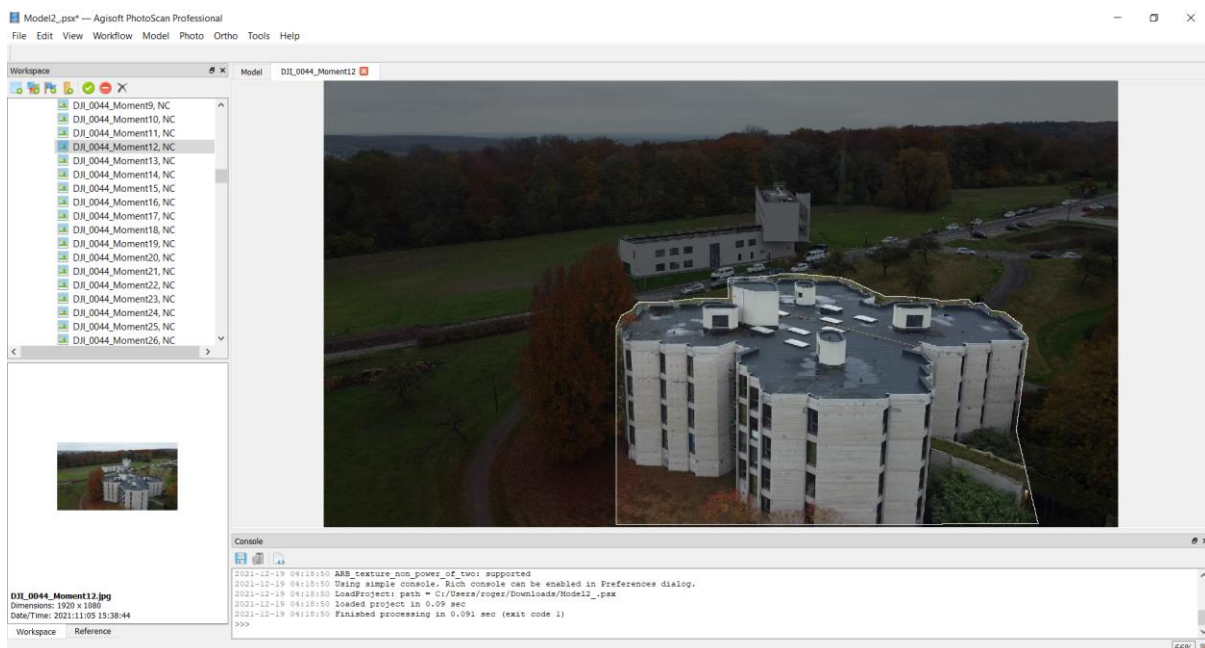
Figure 3-16: Agisoft screenshot. Creating the mask of the building.

3. The next step is to re-align the photos to apply the created masks. This time we set the accuracy to the highest and select to apply the masks in the tie points of the advanced image alignment parameters menu. In this way, as can be seen in Figure 3-17, a point cloud with less background has been obtained. This means that we can now focus the detail on the object we want.
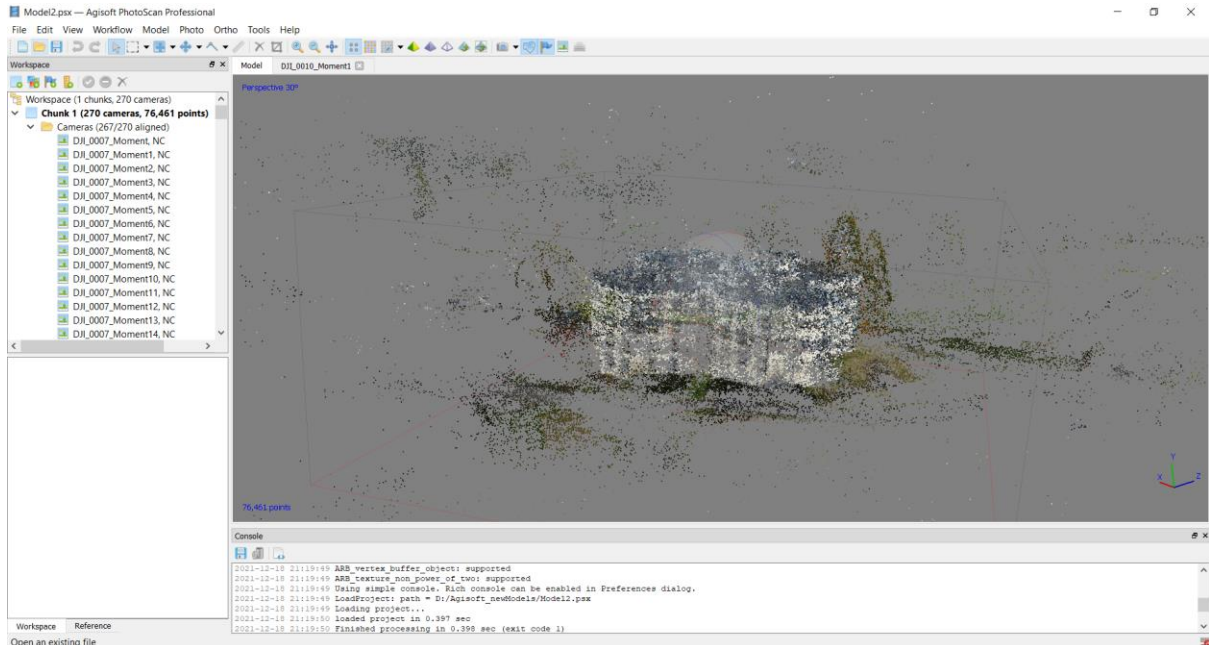
Figure 3-17: Agisoft screenshot. Point cloud with the masks applied.

4. Next, we build a dense cloud. To do this, go to the same workflow menu, select built dense cloud with the quality set to ultra-high and the deep filter set to aggressive. The result is the dense cloud in Figure 3-18.
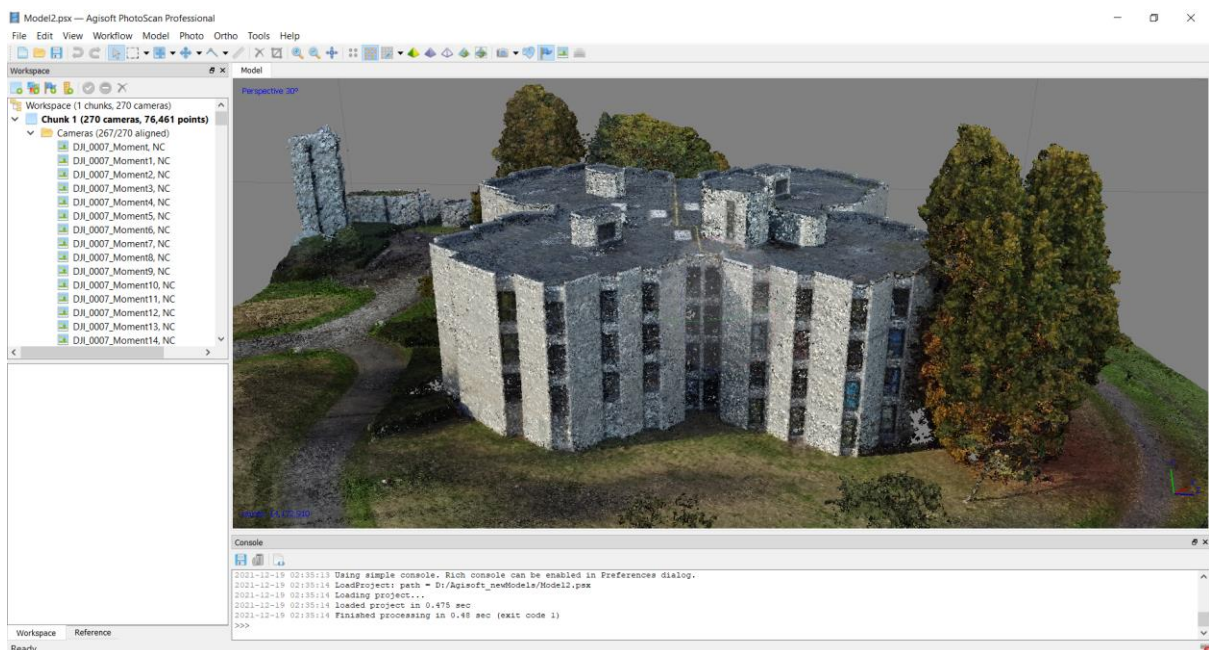
Figure 3-18: Agisoft screenshot. Dense cloud.

5. The next step is to build the mesh. Again we go to the workflow menu, build mesh and set the face count option to the highest. In Figure 3-19, we can see the result after the simulation, the shaded model.
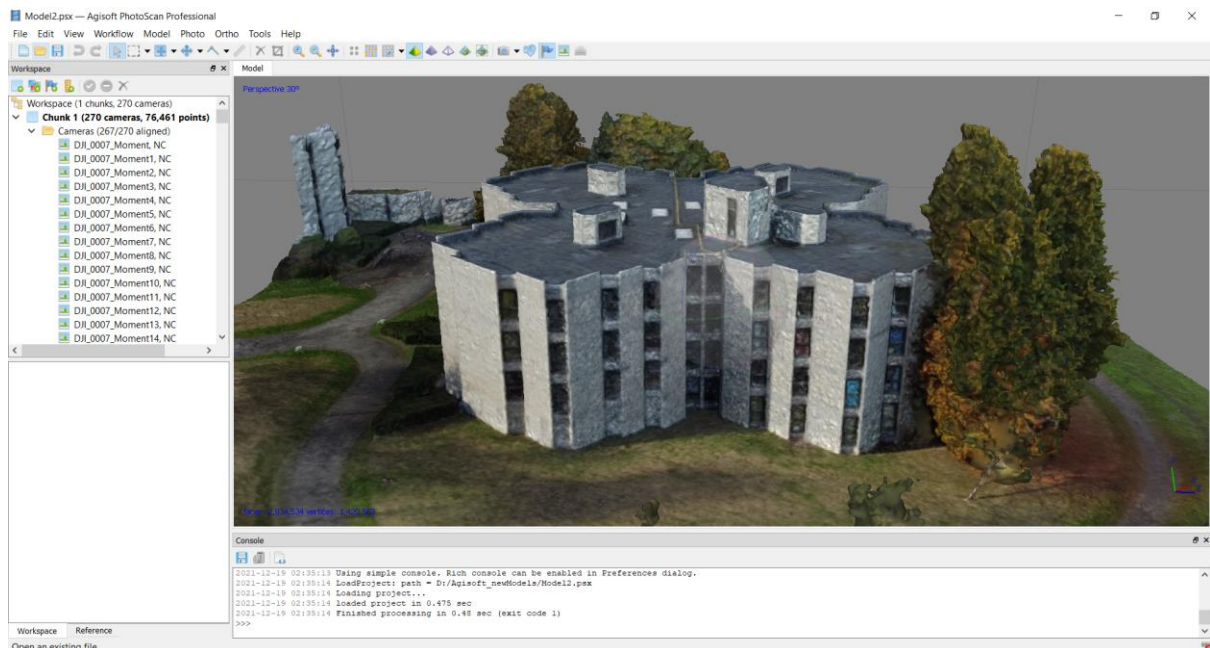
Figure 3-19: Agisoft screenshot. Shaded model.

6. Once the mesh is built, go to the workflow menu and build the texture. This time we leave the default parameters. The texture of the building can be seen in the screenshot in Figure 3-20.
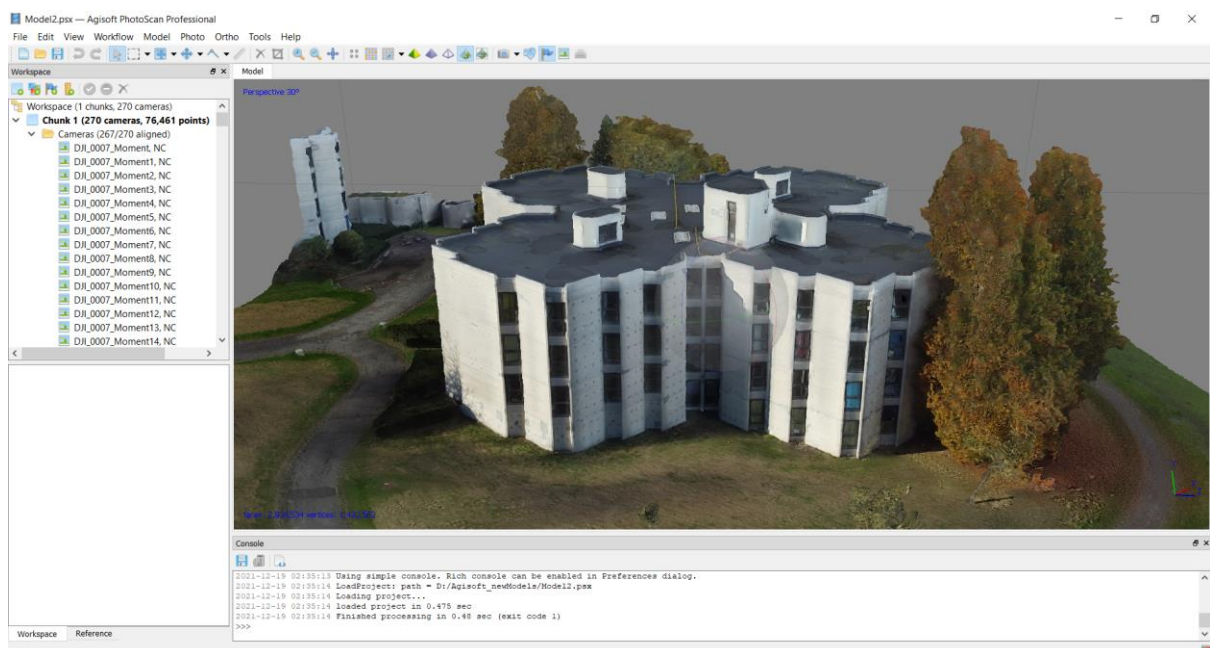
Figure 3-20: Agisoft screenshot. Textured model.

7. The last step with Agisoft will be to build the tiled model. As before, we will select this option in the workflow menu and we will get the more detailed model in Figure 3-21, the tiled model.
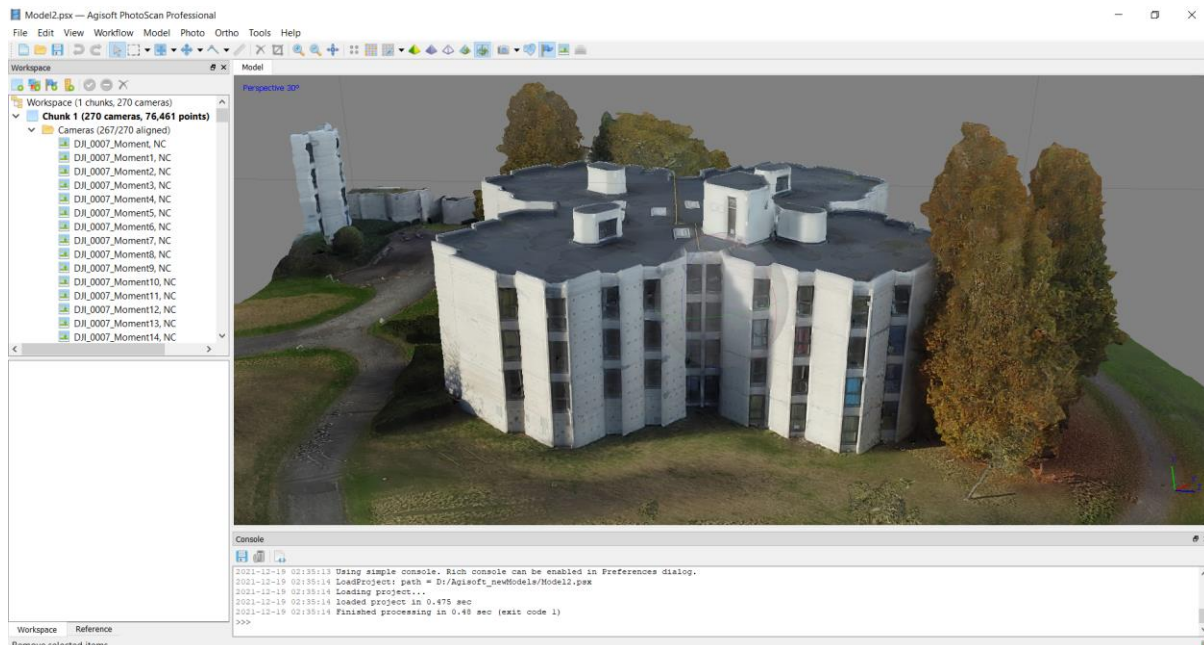
Figure 3-21: Agisoft screenshot. Tiled model.

8. It is time to export our model in .stl format, save it.

Table 3-5 summarizes the parameters selected in Agisoft based on software developer recommendations and test and trial.

Table 3-5: Parameters used in Agisoft Software.

Photo Alignment Parameters	
Accuracy	Highest
Generic reselection	Enabled
Point Limit	126.498
Building dense point cloud	
Quality	Ultra-high
Depth Filtering	Aggressive
Calculate point colours	Enabled
Building mesh	
Source data	Dense Cloud
Surface type	Arbitrary (3D)

Face count	High
Calculate vertex colours	Enabled
Building Texture	
Mapping Mode	Generic
Blending Mode	Mosaic
Texture size/ count	4096 x 1
Enable hole filling	Enabled
Enable ghosting filter	Enabled
Building Tiled Model	
Source data	Dense cloud
Pixel size (m)	0.00596779
Tile size	4096
Enable ghosting filter	Enabled

9. Now, we will import the saved model in .stl format into the 3D modelling software Meshmixer. In Figure 3-22 we can see the 3D model after orienting it well.
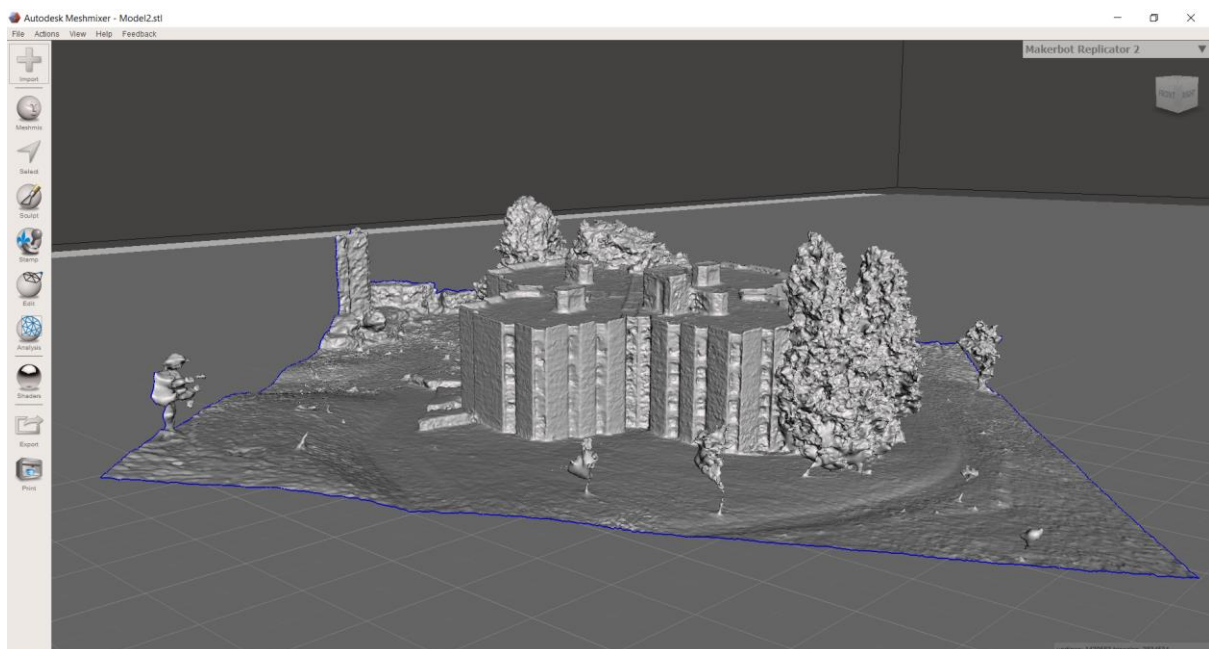
Figure 3-22: Meshmixer screenshot. 3D model imported and oriented.

10. As we only want the building, we will cut out all the objects around it using the Meshmixer editing tools. In Figure 3-23, we can see the cropping process.
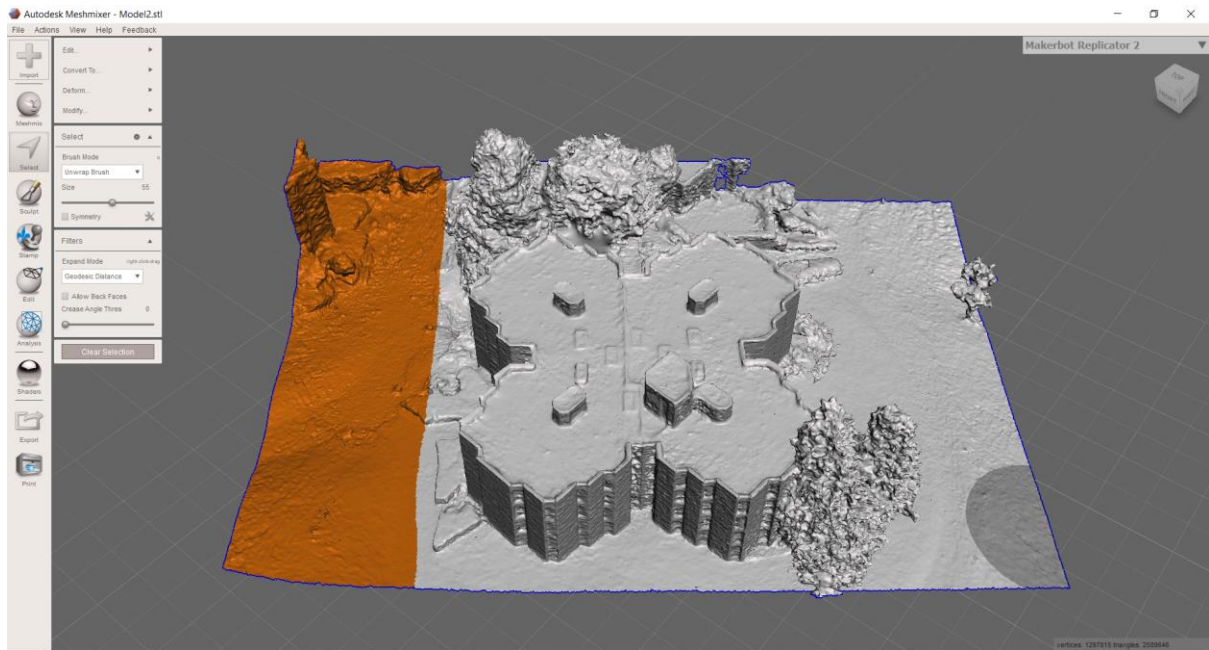
Figure 3-23: Meshmixer screenshot. Cutting process.

We want to get a result like in Figure 3-24 for the next steps.
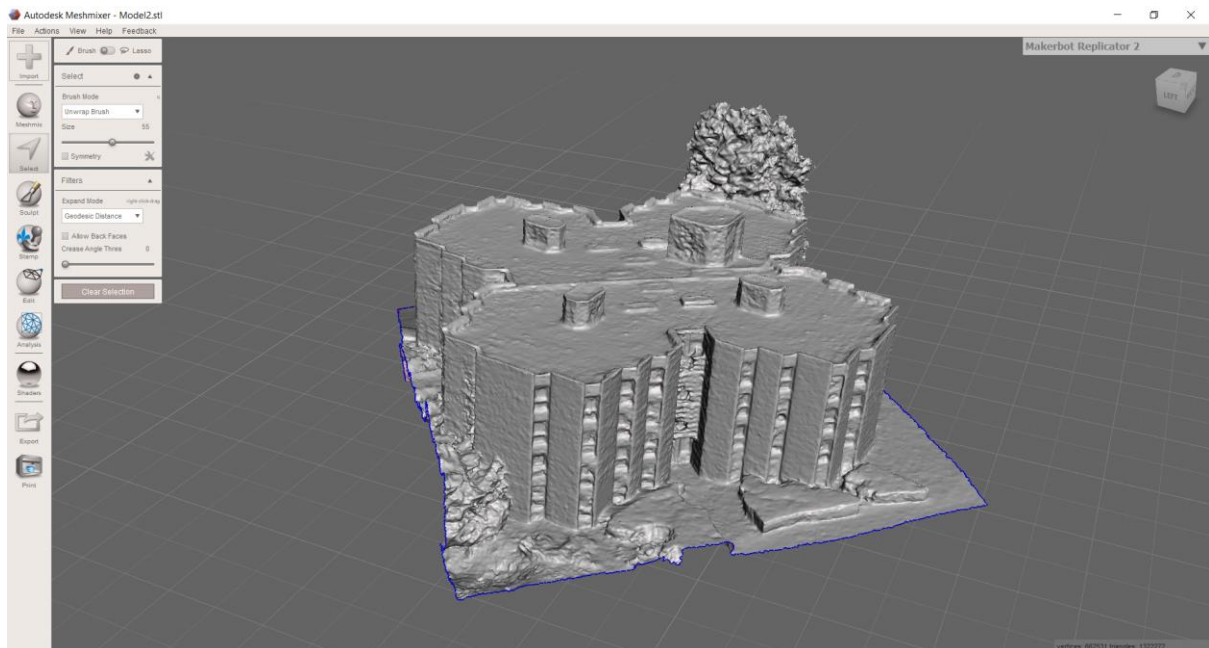
Figure 3-24: Meshmixer screenshot. Model cutted.

11. In the edit menu, we will use the option Make solid with the parameters defined in Table 3-6. In Figure 3-25 we can see a screenshot of the result.

Table 3-6: Parameters used in Meshmixer - Make Solid.

Make Solid	
Solid Type	Accurate
Color Transfer Mode	Automatic
Solid Accuracy	512
Cell Size	0.02 mm
Mesh Density	512
Cell Size	0.016 mm
Closed Open Bondaries	Enabled
Auto-Repair Result	Enabled
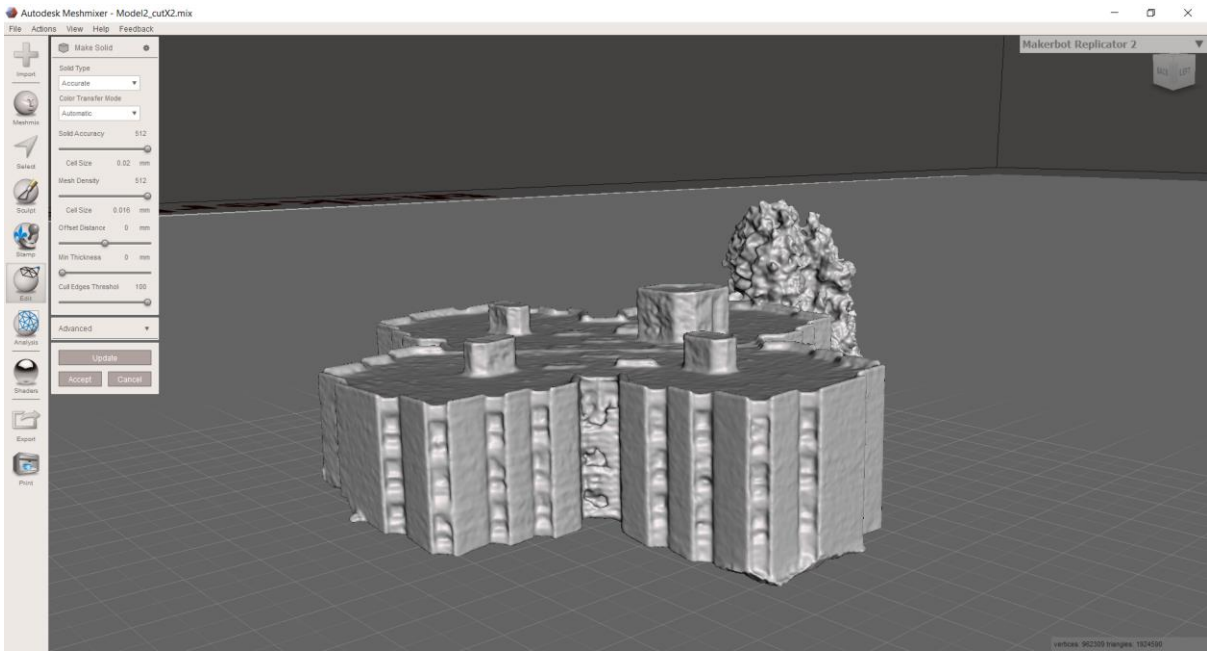
Figure 3-25: Meshmixer screenshot. Solid model.

12. In the last steps, we will edit the solid model to cut and polish irregular shapes that protrude from the facade of the building (Figure 3-26).
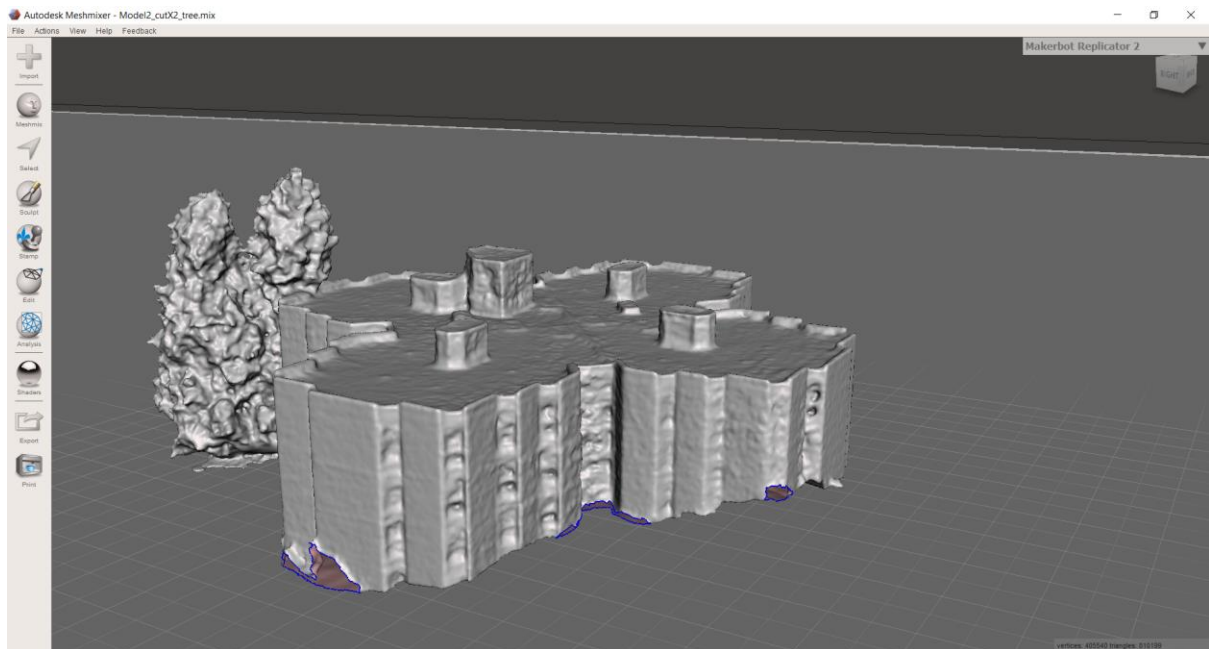
Figure 3-26: Meshmixer screenshot. Cutting and polishing irregular shapes.

13. We will repeat step 11, to make the solid model again and we will also cut the tree attached to the facade with the Plan Cut option. In Figure 3-27, we can see the result once the tree has been cut.
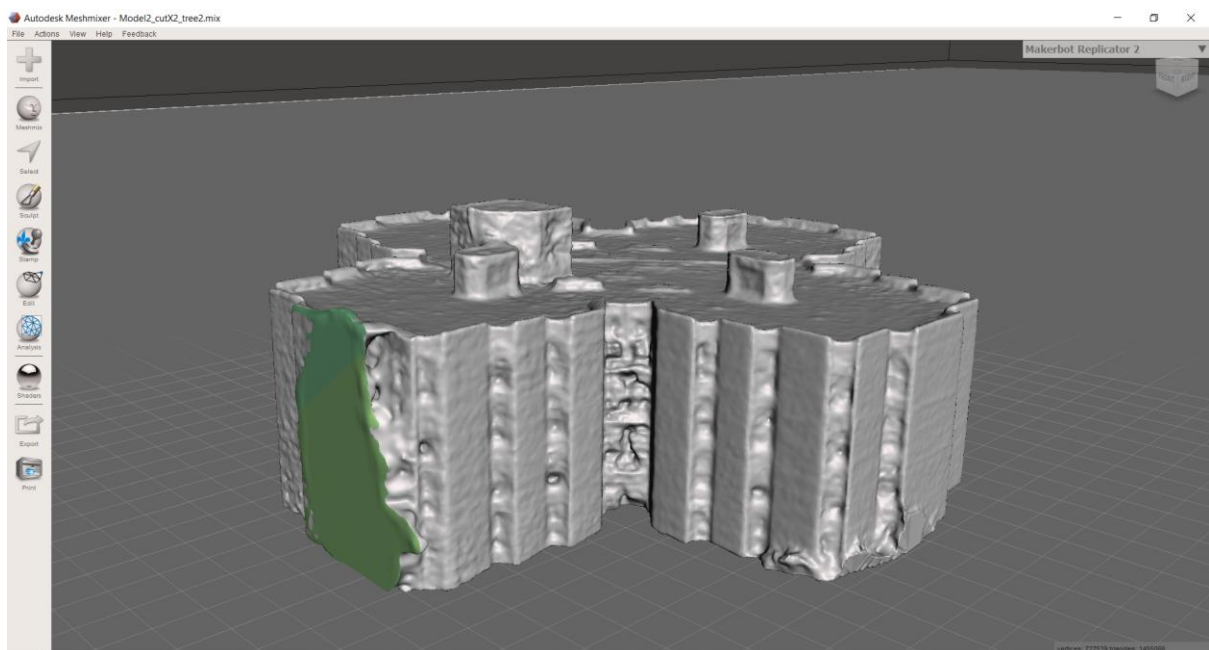
Figure 3-27: Meshmixer screenshot. Solid model with the tree cutted.

14. Finally, using the Plan cut option, we will make the base of the building flat by cutting it with a horizontal plane taking as a reference the lowest point of the facade which allows us to obtain a flat base. In Figure 3-28, we can see the final solid model in Meshmixer software.
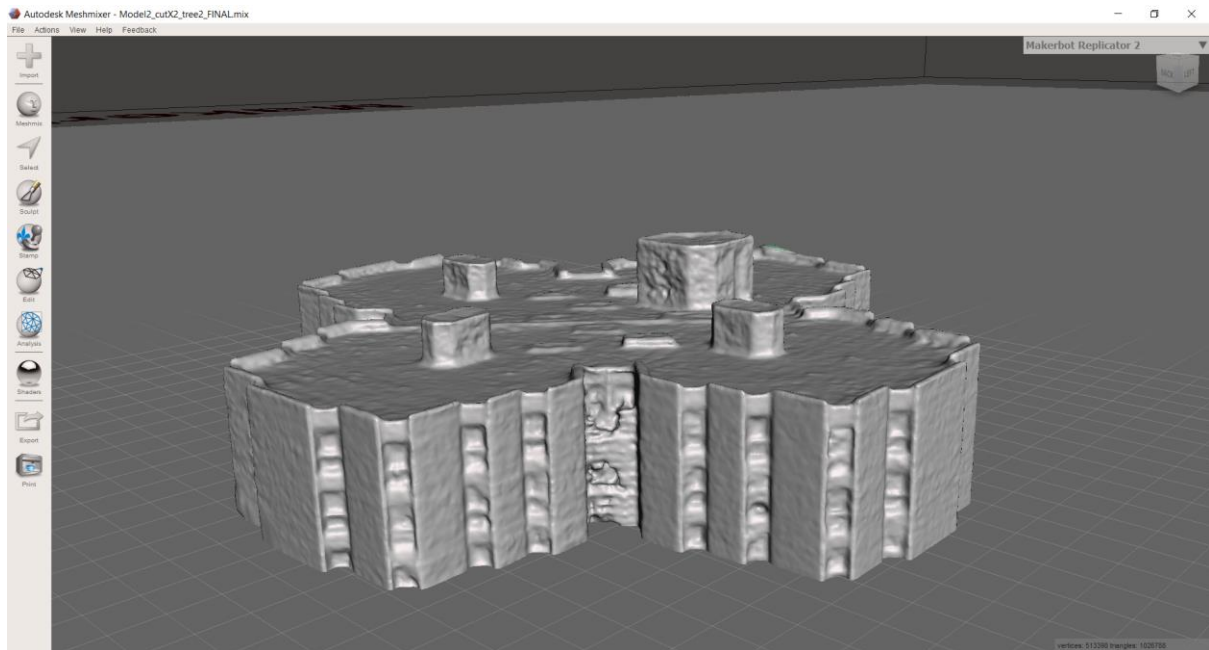
Figure 3-28: Meshmixer screenshot. Final solid model with a flat base.

15. Once we have the solid model ready, we will export it and save it in .stl format. Then we import it into our PrusaSlicer printer software.

16. The first action we will do once we have the imported model is to size it correctly. We will define the longitudinal dimension Y and at 100 mm, in this way, we will get a 10x10cm model with a scale of 1:400. In Figure 3-29, we can see the resized model.
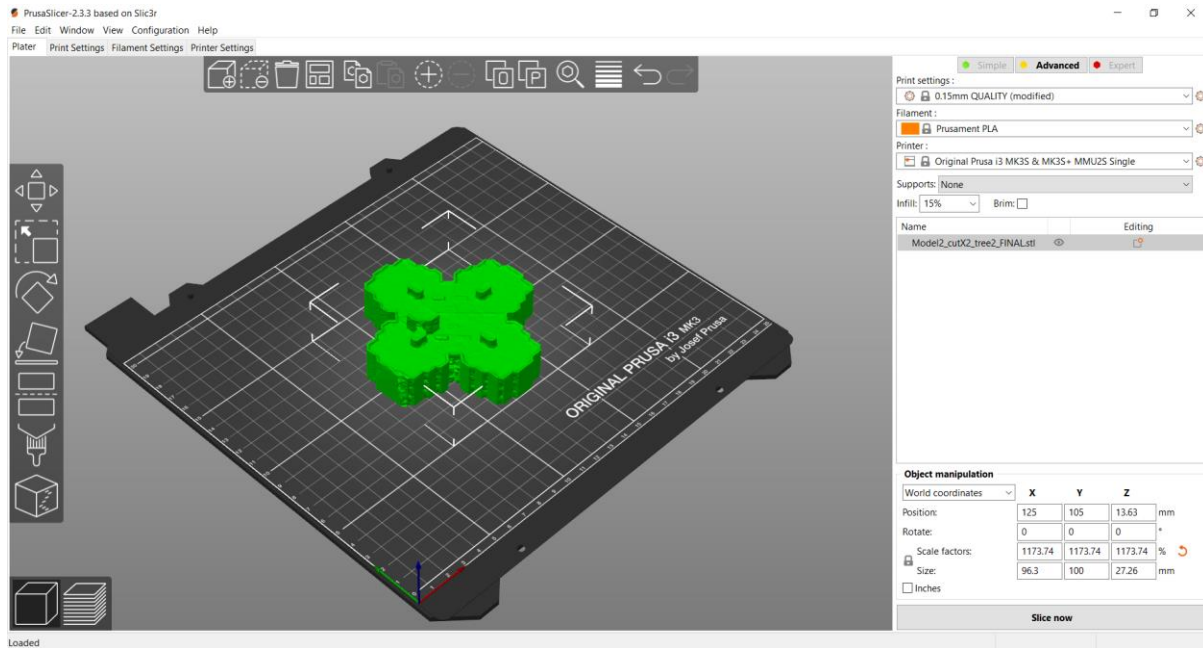
Figure 3-29: PrusaSlicer screenshot. Model imported and resized.

17. The next step will be to slice the model to define the printer passes. We will also define the parameters for printing, such as the size of the filament used, the shape of the internal structure, the lightness or the % of the material used, among others. In Table 3-7, we can see the most relevant defined parameters.

Table 3-7: Relevant 3D printing parameters.

PRINT SETTINGS	0.15 mm QUALITY @MK3
Layer height	0,15 mm
First layer height	0.2 mm
Vertical shells:	
Perimeters	2
Horizontal shells:	
Solid layers - Top	7
Solid layers - Bottom	5
Minimum shell thickness - Top	0.7 mm
Minimum shell thickness - Bottom	0.5 mm
Infill:	
Fill density	15%
Fill pattern	Gyroid
FILAMENT SETTINGS	Prusament PLA
Diameter	1.75 mm

Density	124 g/cm^3
Cost	30.24 money/kg
Spool weight	201 g
PRINTER SETTINGS	Original Prusa i3 MK3S
Nozzle diameter	0.4 mm

In Figure 3-30, we can see the sliced model. It should be noted that the printing time will be 1 h 18 mins and 12.89 m of filament will be used.
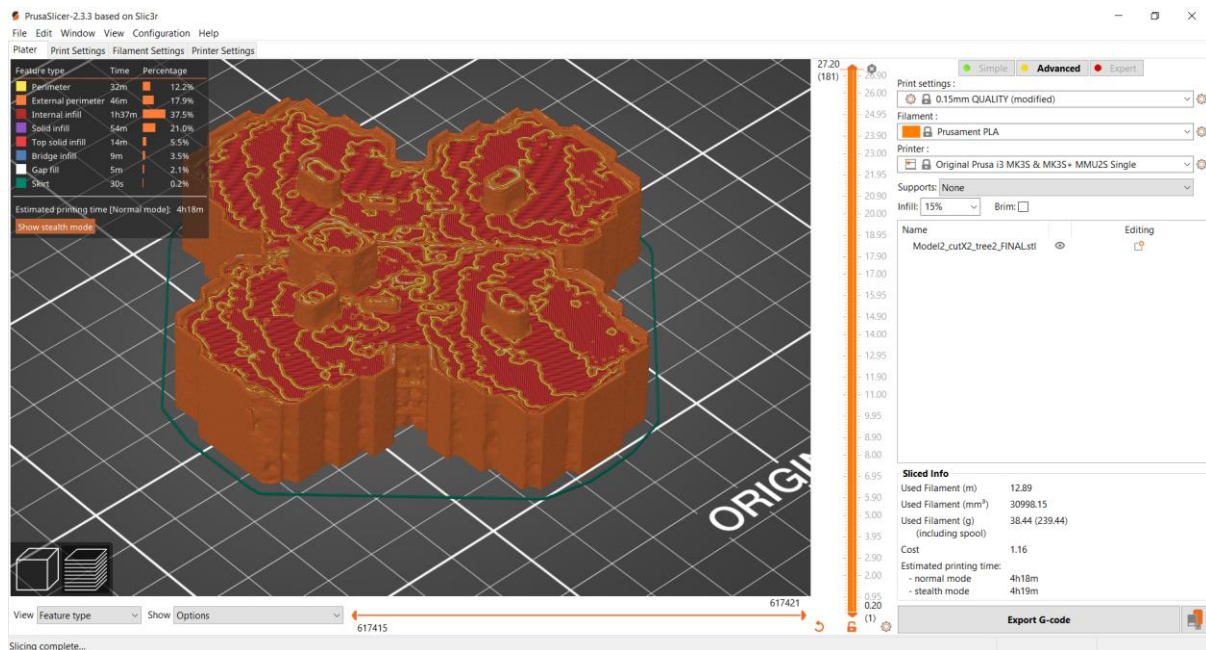
Figure 3-30: PrusaSlicer screenshot. Sliced model.

In Figure 3-31, a middle stage of the impression shows the internal structure of the 3d printing. It corresponds to a Gyroid structure that allows reducing the density of the model to 15% of the material.
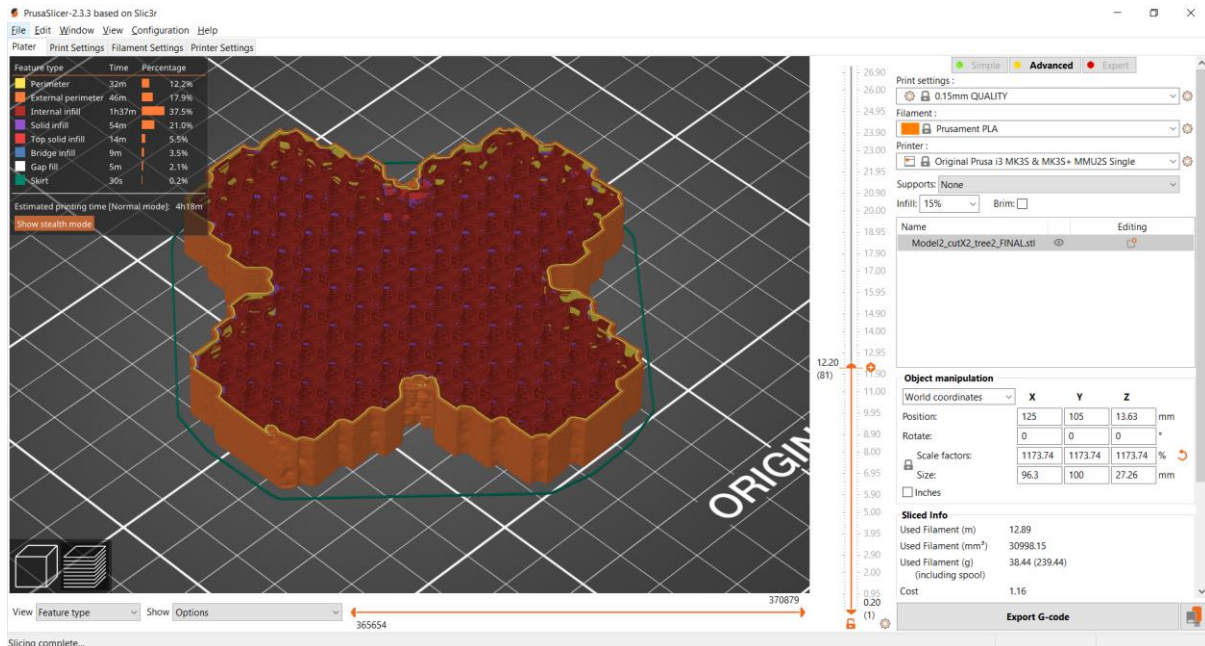
Figure 3-31: PrusaSlicer screenshot. Middle stage of the 3D printing (Gyroid structure).

18. The last step with the PrusaSlicer software is to export the model in G-code. This code will allow us to transfer the print file to the printer via the Pronterface software.

19. Finally, we will import the .g-code file into Pronterface. We will establish a connection with the Original Prusa i3 MK3S 3D printer loaded with enough 0.17 mm PLA filament and start 3D printing. An interesting tip is to put a thin layer of glue on the surface of the printer to facilitate the fixation of 3D printing during printing.

In Figure 3-32, we can see an instant of the printing process where the internal structure with gyroid structure can be clearly appreciated.
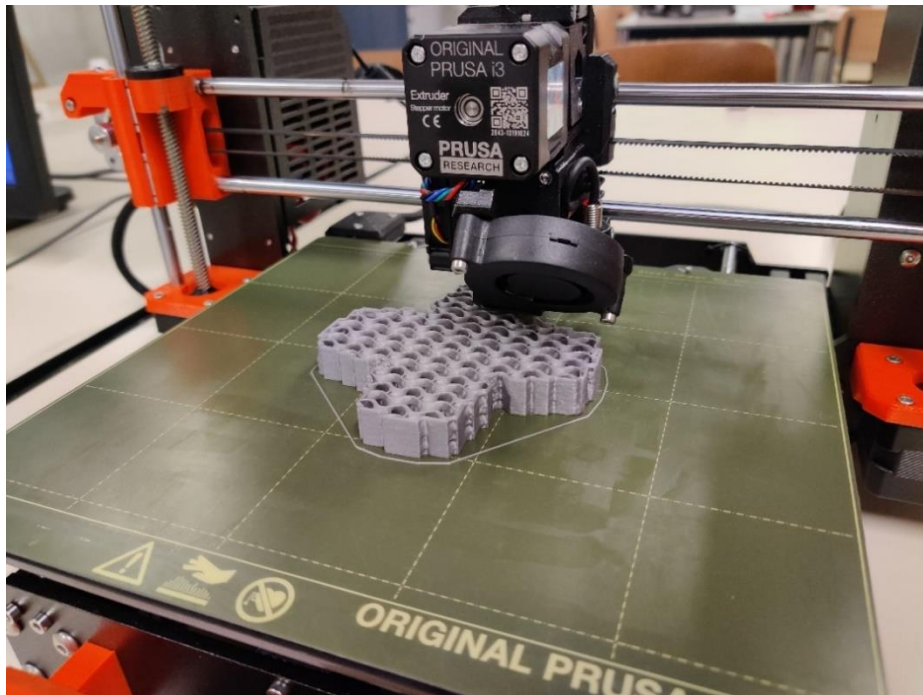
Figure 3-32: 3D printing process with Original Prusa i3 MK3S.

Figure 3-33 shows the 3D printer printing connected to the computer with the Pronterface software on the computer monitor during the printing process.
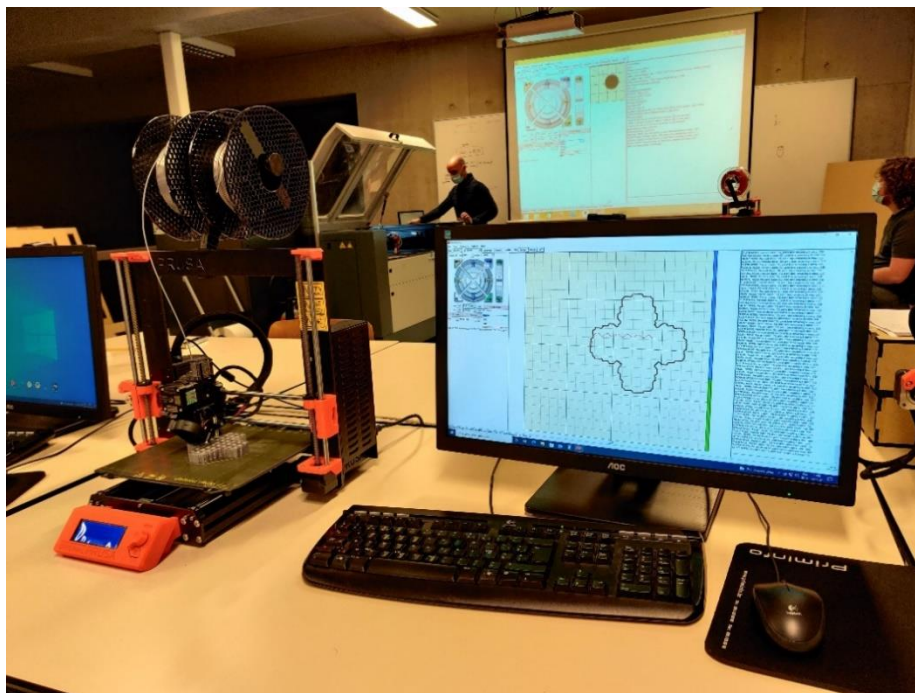
Figure 3-33: 3D printer and computer with Pronterface software during the printing process.

These are the 19 detailed steps we have followed in order to achieve a 3D print from the images obtained by the drone.

3.6 Boundary conditions

In this section, we will explain what the study does and does not cover, the limitations that have been encountered throughout the study and the strategies that have been followed to overcome these limitations.

In this study, we measured the thermal transmittance (U-value) of the wall of room D106, on the ground floor of the southeast tower of building B13A of the university residence of the University of Liège. Therefore, all measurements of the parameters necessary to obtain the U-value have been carried out in this room. Specifically, these measurements correspond to the installation of the heat flux sensor kit for the real-time monitoring of the U-value, as well as the measurements of different ambient and surface temperatures for the estimation of the U-value from thermal images. Also, in the calculations of the thermal transmittance of the wall according to the standards, we have looked for the composition of the wall of the same room, which is the same for all the walls of the rooms of the building.

It should be taken into account that we had limited time to carry out the study and to obtain data, which means that it was not possible to take more measurements to contrast the data obtained, which could have been interesting. It should also be noted that it was not easy for us to access the rooms in the building, as it is fully occupied by students living there, and we were only able to obtain measurements from the room mentioned above. However, we overcame these limitations and managed to obtain the necessary data to obtain good results for this study.

Another relevant aspect is the fact that we have not been able to have a drone with a thermal camera, as a UAP of these characteristics has a high cost and requires driving licences. To overcome this shortcoming, we have chosen to use a small drone capable of obtaining good images of the building. In this way, we were able to make a 3D model of the building and print it on a 3D printer to validate the accuracy of the method and implement a 3D modelling methodology. This method can serve as a basis for future researchers interested in the field and with the availability of a UAP with a thermal camera. Concerning the acquisition of thermal images, we have used a hand-held thermal camera. It does not have a very high resolution but it has allowed us to obtain infrared images of the building to estimate the U-value and to identify the stains of the building envelopes.

3.7 Quality criteria

In this section, we will describe the quality criteria we have followed in our study and we will also discuss the reproducibility of the methodology used in this work.

Concerning the methods of calculation and approximation of the thermal transmittance of the building walls, real-time monitoring has been used as a base value, as it is the most reliable method and the closest to reality. This method allows us to obtain a real reading of the U.value of the walls following the conditions imposed by the ISO 9869 standard. For this reason, in the calculation of the u-value according to the standards

and the estimation of the u-value through thermal images, the value obtained with the real-time monitoring has been taken into account as a value to be approximated.

Regarding 3D printing, in order to assess the quality of the method, we will focus on analysing the accuracy and degree of definition of the 3D print by comparing it with the real building. In this way, we will draw conclusions of the methodology developed and if it can serve as a basis for a 3D model with thermal drones for possible future work.

This work has a high degree of reproducibility, as the software used, the equipment used and the standards followed are described in detail throughout the work. The method followed in all the calculations and tests carried out is also explained in detail.

The software used are Agisoft PhotoScan Professional, Meshmixer, PrusaSlicer and, Pronterface, presented in more detail in section 3.5.4. As for the equipment used, they are the gSKIN® U-Value Kit, the FLIR i7 hand-held thermal camera, the DJI mini 2 drone, the Workstation with 64 cores and the Original Prusa i3 MK3S 3D printer. These devices are described in their corresponding chapter throughout sections 3.4 and 3.5. Finally, the standard mainly followed is ISO 9869.

You can follow the procedures used in this work throughout Chapter 0 of Methodology.

4 Results

In this chapter, we present the results obtained following the methodology described in Chapter 3. These results will be used to answer the research questions raised, which are set out below:

- How to get a 3D model and a 3D printed maquette of a building through pictures obtained from a drone?

- How to estimate the values of thermal transmittance (U-value) of a building envelope using thermal images?

- How do the U-values obtained from (i) real monitoring using heat flow sensors, (ii) calculation method according to the standard ISO 9869, and (iii) estimations based on thermal imaging differ in terms of accuracy, speed, cost, and usability?

First of all, we show the results of the thermal transmittance value (U-value) of the wall of the residence building of the University of Liège, obtained by the methods described above: real-time monitoring, calculation according to the relevant standards and estimation based on infrared thermography. After that, we present a comparison of the three methods. With this, we will answer the second and third research questions.

Then, we also show the result of the 3D printing of the building, which is the final result of the methodology asked by the first research question.

4.1 U-value real-time monitoring

Through the gSKIN® U-Value Kit, we have obtained values of the indoor temperature, outdoor temperature, heat flux and thermal transmittance of the building for every minute during 72 hours. These results are shown in Figure 4-1. Where each parameter is represented by a line. The report given by the software is shown in Annex 6.
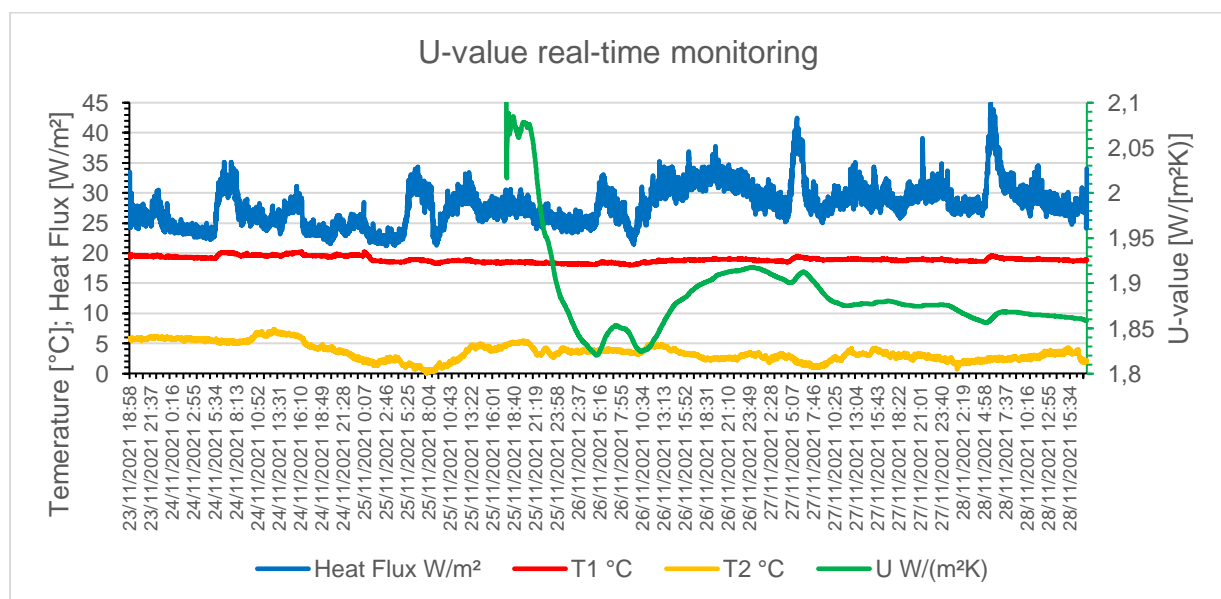

Figure 4-1: U-value real-time monitoring.

The logger data collected from our measurement are shown in Table 4-1:

Table 4-1: Logger data.

Type	U-value measurement kit
Sensitivity	11.9 uV/(W/m^2)
Inside temp. (T1)	18.9 ºC
Outside temp. (T2)	3.5 ºC
Measurement time (t)	118.73 h

Table 4-2 contains the results of U-value analysis using the average method (ISO 9869-1:2014):

Table 4-2: U-value analysis using the average method.

Analysis start time	2021-11-25 17:42:44
Analysis end time	2021-11-28 17:42:44
Analysis period	72 h
U-value	1.86 W/(m^{2}K)
U-value w/o last 24h (U24)	1.88 W/(m^{2}K)
dU24	-1.1 %
dR24	1.6 %

Through real-time monitoring, a U-value of 1.86 W/m^2·K has been obtained.

Observing the results, we can indicate that the conditions of ISO 9869-1:2014, as described in section 3.5 Data analysis, are fulfilled and are as follows:

- The temperature difference is more than 5 ºC between inside and outside, as the average indoor temperature is 18.9 ºC and the average outdoor temperature is 3.5 ºC.

- The sensors have been functional throughout the monitoring period.

- The measurement time was 118.73 h, exceeding 72 h. U-value data has been collected during the last 72 h.

- The last measured U-value has differed less than 5% from U-value 24h before, specifically, it has differed -1.1 %.

- The temperature curves have not crossed at any time as we can see in Figure 4-1, where the yellow curve corresponds to the inside temperature and the red curve to the outside temperature.

A U-value of 1.86 W/m^2·K is a very high thermal transmittance value which indicates that the insulation of the walls is not working properly. This is a logical result as we are analysing a building constructed in the 1960s, i.e. more than 50 years old, and it may well be that the insulation has degraded over time or is wet due to possible rainwater

seepage. Therefore, we can say that this is a good result very close to reality and confirms once again that the real-time monitoring has been carried out correctly.

4.2 U-value calculation according to the standards

The results of the calculation of the U-value of the wall following the standards ISO 9868-1:2014, using equations (*1*), (*2*) and (*3*) explained in section 3.4.2, were as follows.

First, the values of the thermal resistances of the wall layers and the total resistance, calculated with Equation (*3*) and (*2*), and summarized in Table 4-3, ordered from the inside to the outside of the building, are shown.

Table 4-3: Results of calculation accoding to ISO 9869.

R_{si}	0.13	$(m^2 \cdot K)/W$
R_1 (Concrete - 12 cm)	0.07	$(m^2 \cdot K)/W$
d_1	0.16	m
λ_1	0.035	$W/(m \cdot K)$
R_2 (Insulation rock wool - 7 cm)	2.00	$(m^2 \cdot K)/W$
d_2	0.07	m
λ_2	2.30	$W/(m \cdot K)$
R_3 (Concrete - 16 cm)	0.05	$(m^2 \cdot K)/W$
d_3	0.12	m
λ_3	0.035	$W/(m \cdot K)$
R_{se}	0.04	$(m^2 \cdot K)/W$
R_T	2.29	$(m^2 \cdot K)/W$
U-value	0.46	$W/(m^2 \cdot K)$

Finally, we use equation (*1*) to calculate the U-value. We obtain a value of 0.46 $W/m^2 \cdot K$. This value is quite good, but if we compare it with the value obtained with the real-time monitoring of 1.86 $W/m^2 \cdot K$ given in section 4.1 above, it shows that it does not match the reality of the wall at this moment. This fact shows that the insulation of rock wool is not working at all correctly. We can be sure that the insulation has a major degradation or humidity problem caused mainly by the passing of the years since the building was constructed.

We repeat the calculations to approximate the value of 1.86 $W/m^2 \cdot K$ obtained through real-time monitoring in section 4.1 above. To solve for this value, we change the thermal conductivity of the rock wool insulation, as we have shown that it is not in good condition and that the thermal conductivity value used is not the actual value. The data is summarised in Table 4-4.

Table 4-4: Results of calculation following ISO 9869 changing λ₂.

R$_{si}$	0.13	(m^2·K)/W
R$_1$ (Concrete - 12 cm)	0.07	(m^2·K)/W
R$_2$ (Insulation rock wool - 7 cm)	2.00	(m^2·K)/W
d$_2$	0.07	m
λ$_2$	**0.285**	**W/(m·K)**
R$_3$ (Concrete - 16 cm)	0.05	(m^2·K)/W
R$_{se}$	0.04	(m^2·K)/W
R$_T$	0.54	(m^2·K)/W
U-value	1.86	W/(m^2·K)

As we can see, with a thermal conductivity value of 0.285 W/m·K for the thermal conductivity of the insulation in a degraded state, we reach the target U-value.

4.3 U-value estimation from thermal imaging

To estimate the value of the thermal transmittance of the walls of the analysed building, we have used the estimation made by (Bayomi et al., 2021). Following the equation (*4*) presented in chapter 3.5.3, we present below the values used (Table 4-5).

Table 4-5: Data used for U-value estimation IRT.

ε	**Emissivity**	0,95	
σ	**Stefan-Boltzmann constant**	5.67x10-8	W·m^{-2}·K^{-4}
T_{refl}	**The apparent measured temperature**	276.25	K
$T_{s,in}$	**Interior wall surface temperature**	290.65	K
$T_{s,out}$	**External wall surface temperature**	279.75	K
h_c	**Convection Coefficient**	8.7	W/(m^2·K)
T_{in}	**The indoor air temperature**	292.71	K
U-value	**Thermal transmittance (U-value)**	1.64	W/(m^2·K)

We obtain an estimated U-value of 1.64 W/m^2·K. We would like to emphasise that this equation is very sensitive to the inner surface temperature of the wall, as it appears in three terms of the equation. For this reason, this equation has to be used with caution.

With this result close to the value obtained in section 4.1 by real-time monitoring of 1.86 W/m^2·K, we can conclude that we have found a method to estimate the thermal conductivity quantitatively with caution and, we can therefore answer the second research question.

We have also carried out a qualitative estimation of the thermal transmittance. This estimation is based on analysing the thermal images of the captured building envelopes. The objective is to find thermal anomalies on the facades of the residence in order to detect possible problems. These problems can be for example thermal bridges, material degradation along the walls or insulation degradation. The software FLIR Thermal Studio was used to analyze temperature readings from approximately 90 images, as shown in Figure 4-2.
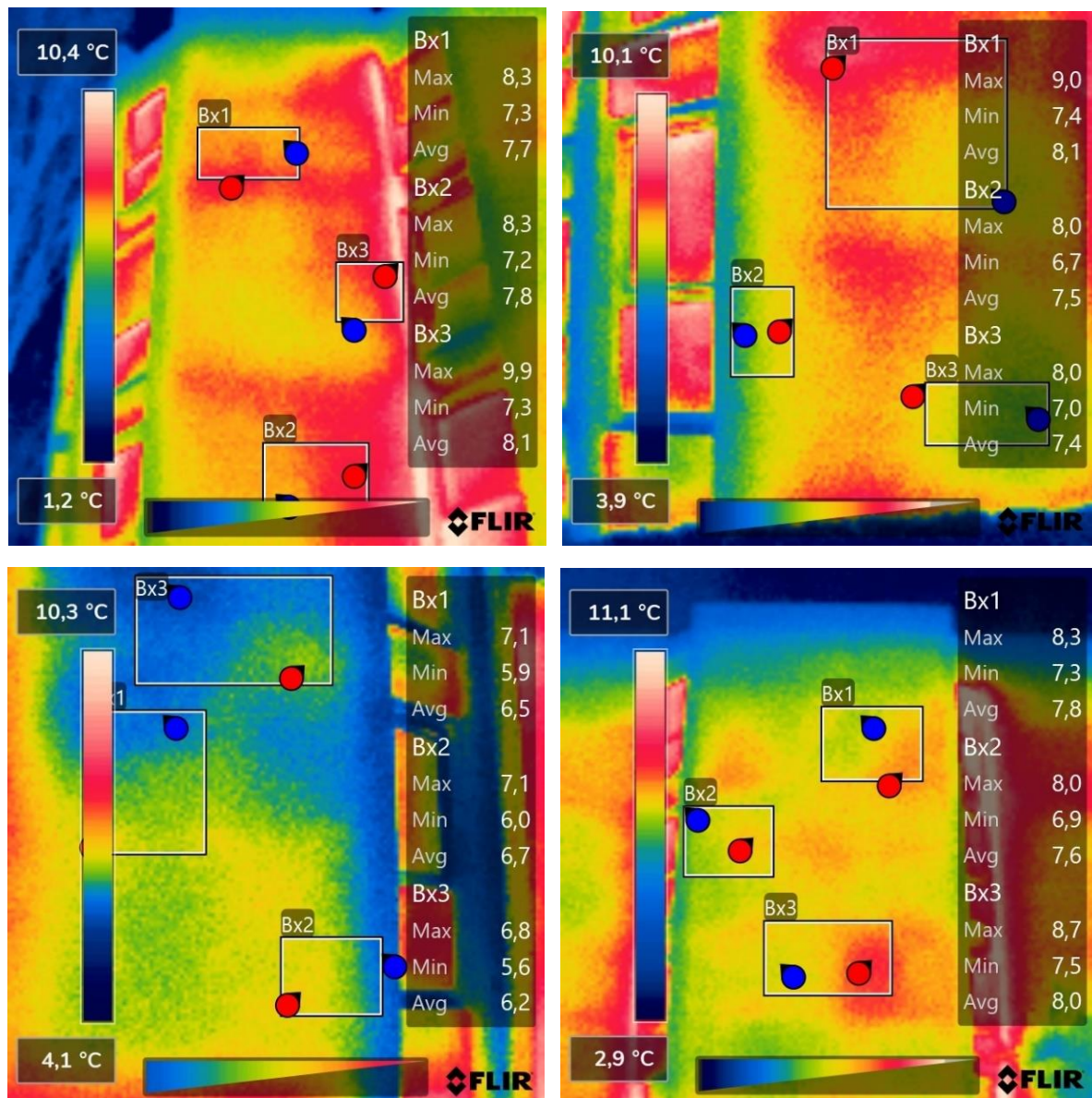

Figure 4-2: Sample of thermal imaging analysis.

The results of the thermal image analysis reveal 3 types of anomalies in the assessed building: thermal bridge, material degradation and insulation failures. The distinction of the three types of anomalies is based on the location and the shape of the anomaly. Thermal bridging was identified as vertical or horizontal anomalies located between

floors and around the corners of the building. Deterioration of the façade material involves the degradation of the cladding materials or the presence of cracks. Finally, insulation failure leads to thermal leakage around windows and cracks and degradation of insulation along the building envelope. This anomaly is identified when temperature differences of 2 degrees are detected along the same wall.

4.4 Comparison of methods for obtaining the U-value

In this chapter, we have made a comparison of the different methods used in this study to obtain the value of the thermal transmittance (U-value). Specifically, we compare the results obtained in section 4.1 U-value real-time monitoring, 4.2 U-value calculation according to the standards and, 4.3 U-value estimation from thermal imaging. In order to make this comparison, we have based ourselves on 4 terms which are set out below:

- Accuracy: approximation to the real value of thermal transmittance. We have calculated the percentage deviation of the U-value of each method from the U-value obtained from real-time monitoring, as this is the most accurate method.

- Speed: time used to obtain the U-value. It includes the estimated time of measurement of parameters and calculations performed on a case-by-case basis.

- Cost: estimation in Euros of the total cost of the equipment used. Does not include the cost per hour of the user performing measurements or calculations.

- Usability: ease of carrying out the method undertaken for the calculation or estimation of the U-value.

In Table 4-6, we compare each method (row) with each comparison term (column).

Table 4-6: Comparison of U-value methods.

	U-value [W/m²·K]	Accuracy	Speed	Cost	Usability
Real-time monitoring	1.86	Very high accuracy. It measures the actual U-value of the wall according to the requirements of ISO 9869.	73 h The minimum 72 hours required for real-time monitoring plus one hour to install the sensors correctly on the wall are considered.	1,733.22 € Cost of gSKIN U-Value Kit without taking border taxes into account.	Complex usability. Complexity to install the sensor kit correctly on the wall, as certain conditions must be respected to meet the requirements.
Calculations according to the standards	0.46	Very low accuracy. The calculation was made on the assumption that the wall materials are in perfect condition. 76.54% deviation from the U-value obtained by real-time monitoring.	1 h Estimated time to be spent to perform U-value calculations.	0 €	Easy usability. Simple calculations are required.
Estimation from thermal imaging	1.64	Good accuracy. The estimate of the U-value gives a fairly close estimate of reality. 11.60% deviation from the U-value obtained by real-time monitoring.	2 h One hour has been estimated to measure all temperatures required for the estimation and one hour to perform the calculations.	881.40 € Approximate market price of the FLIR i7 thermal camera used for the estimation. Other thermal cameras can be used.	Medium usability. Some complexity in the correct measurement of wall surface temperatures and reflection temperature, as temperatures can easily vary. Ease of following the estimation equations.

If we look at the accuracy of the methods, the most reliable and accurate method is real-time monitoring. This method provides us with a very accurate value of 1.86 $W/m^2 \cdot K$, as it measures the thermal transmittance of the real wall following the requirements of the ISO 9869 standard, as described in section 3.4.1. For this reason, we have considered this value as the reference value to compare the accuracy of the other methods.

The calculation of the U-value according to ISO 9869 standards, the second method in Table 4-6, gives very poor accuracy with a value of 0.46 $W/m^2 \cdot K$ and with a deviation of 76.54% from the reference value. This is a very technical method that assumes that the wall materials are in perfect condition, which is far from the reality of the building.

Regarding the estimation from thermal images, we obtained a value of 1.64 $W/m^2 \cdot K$. We can say that this value has a good accuracy as the deviation from the reference value is 11.60%. However, this method is very sensitive to the temperature of the inner surface and must be used with caution as the results can be very different from reality.

In terms of speed, the most time-consuming method is real-time monitoring, which requires a minimum measurement of 72h. On the contrary, the fastest method is the standard calculation method with an estimated 1h followed by the estimation from thermal images with 2h.

Looking at the cost of each method, real-time monitoring is the most expensive, as the sensor equipment used costs more than 1,700 € without taking into account border fees. For the estimation from thermal images, we have used a thermal camera which costs approximately 881.40 €. The calculation of the U-value according to the standards has a zero cost as no equipment is needed.

Finally, as far as usability is concerned, real-time monitoring is the most complex system as it is easy to make mistakes in the installation of the equipment because it requires several parameters to be taken into account, so we have defined this method with complex usability.

The other two methods are simpler since they require little more than a correct procedure to perform the calculations. It should be noted that the estimation through thermal images requires a correct collection of surface temperatures with the thermal camera, which can differ due to the presence of humidity or rain for example. For this reason, this method has been classified as medium usability.

To summarize, the most accurate method is real-time monitoring, but it requires more time, costs more, and is more complex than other methods. Quite the opposite of the calculation according to the standards, which has very poor accuracy but requires the least in the other terms. Finally, the estimation from IRT is between the other two methods, which with a very short time we can achieve accuracy close to reality.

4.5 3D printing

Once all the methodology presented in point 3.5.4 of this work has been carried out, we have obtained a 3D impression of the building at a scale of 1:400.

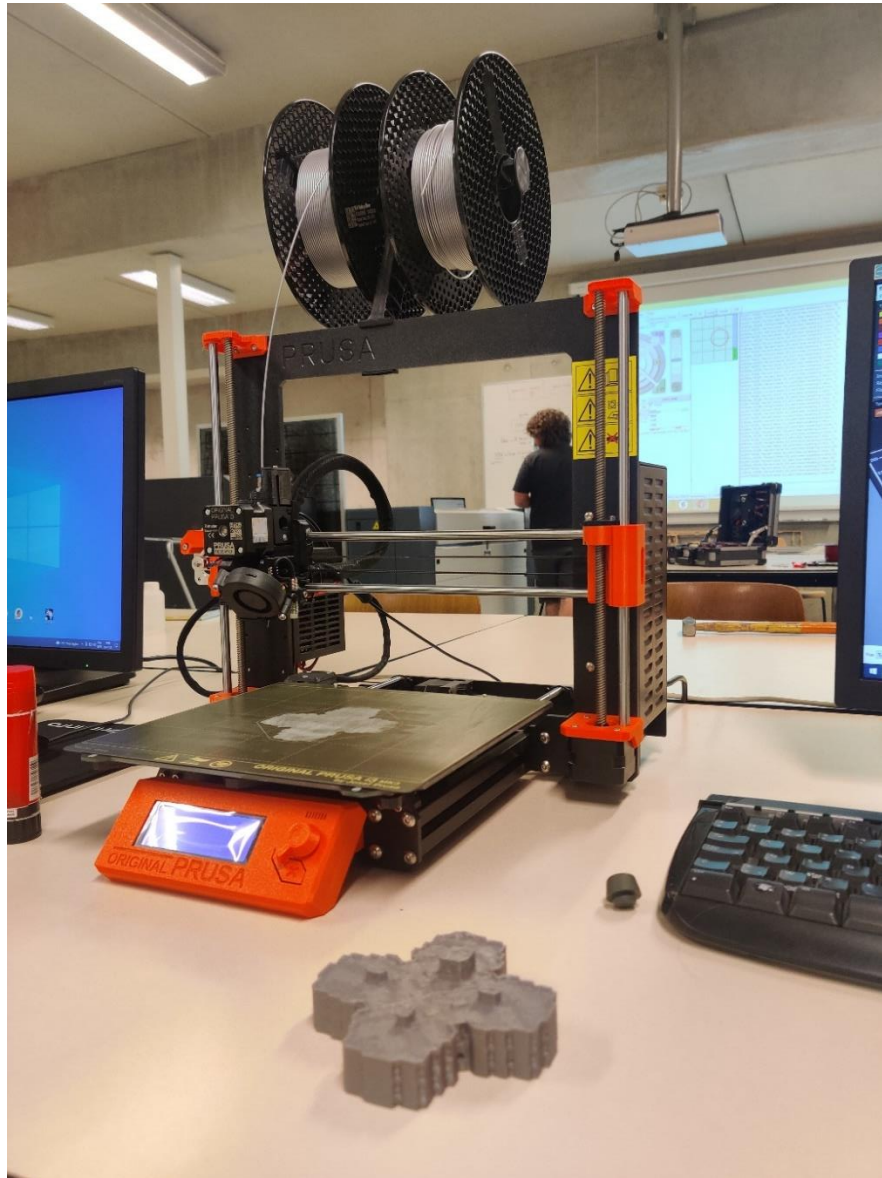Photographs of the 3D printing maquette are shown in the following pictures below.

Figure 4-3 shows the 3D impression of the building with the real building in the background.

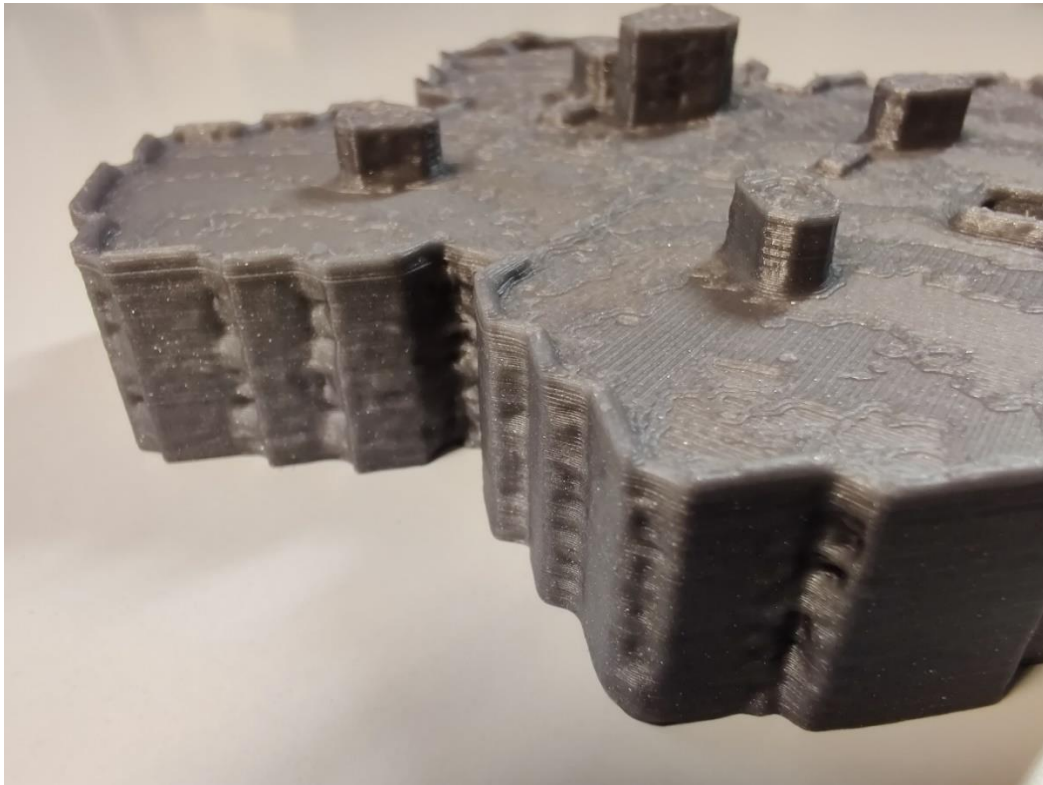*Figure 4-3: 3D printing whit the real building in the background.*

Figure 4-4 shows the 3D print in front of the Prusa printer used.

Figure 4-4: 3D print and Prusa 3D printer.

Finally, in Figure 4-5 and Figure 4-6 we can see the 3D printed model of the building up close where you can see the details.

Figure 4-5: 3D printing details.

Figure 4-6: Complete 3D maquette.

Analysing the final result of the 3D printing, we can see that in general, we have obtained a model very close to reality.

If we analyse the model in-depth, we can see that there are specific elements that are not very well defined, such as the windows. One of the causes may be that the images of the building were captured at a certain distance from it, thus preventing a very precise definition of specific elements such as the windows. As far as the walls of the façade are concerned, a high degree of accuracy has been obtained, as they are well oriented and very flat.

If we look at the roof of the building, the contour step of the roof has been very well defined, unlike the surface which has a slight relief in the form of water due to the roughness of the 3D virtual model.

In one corner of the building, there was a tree, which we cut down precisely, but the shape of the façade has been lost very slightly.

Finally, we have encountered the problem that the building is located on land with some unevenness. This has meant that the facades of the building are not the same height around the perimeter of the building. For this reason, our virtual 3D model had a non-flat irregular base. In order to get a flat base of the building, we had to cut the building to a certain height, which made us lose some floors of the building in the 3d printing.

5 Discussion

This chapter mainly reflects on the results obtained in this study. First, the restatement of the study proposal is presented, where the main findings obtained in chapter 4 Results will be dealt with and which will generate the answers to the research questions posed throughout this memory. The findings and recommendations based on the results obtained are then presented. The strength and limitations of the study are also discussed. Finally, the last subchapter discusses the implications for the practice of the study and future work.

5.1 Restatement of Study Purpose

The purpose of this work was to evaluate the thermal transmittance of a building envelope based on a mixed approach. This approach mainly involves making an estimate of the thermal transmittance (U-value) from infrared images and comparing and validating this estimate with other methods of obtaining the U-value, such as real-time monitoring and calculation according to standards. This study allows the evaluation of envelopes of buildings built during the 1960s that show high heat losses due mainly to their deterioration (Attia et al., 2021).

As explained in chapter 1, this study aims to develop a methodology to serve as a basis for future projects based on the exploration of building envelopes with drones equipped with thermal cameras. As it is not possible to have a drone with this equipment, it has been decided to use a drone with a normal camera to develop a 3D model and print it with a 3D printer to evaluate the efficiency and accuracy of the method. This part of the work is intended to be the first base for future research work with thermal drones in our laboratory.

The aim of this study is to answer the research questions posed, which are as follows:

- How to get a 3D model and a 3D printed maquette of a building through pictures obtained from a drone?

- How to estimate the values of thermal transmittance (U-value) of a building envelope using thermal images?

- How do the U-values obtained from (i) real monitoring using heat flow sensors, (ii) calculation method according to the standard ISO 9869, and (iii) estimations based on thermal imaging differ in terms of accuracy, speed, cost, and usability?

To answer the first question on how to obtain a 3D printing of a building from images obtained from a drone, we have elaborated a detailed methodology in chapter 3 of the methodology. Specifically, in section 3.5.4 we have described the equipment used and a total of 19 steps starting with the photographs of the building and ending with the 3D print.

The equipment used consists of a workstation with a high processing capacity, used to process the 3D model of the building thanks to the alignment of the images, and a 3D printer model Original Prusa i3 MK3S. Not forgetting the DJI Mini 2 drone presented in section 3.4.4 with which we have captured the images of the building.

The main ideas of the method described in section 3.5.4 are as follows:

- Image alignment and processing with Agisoft Metashape software. Creation of masks on the images to define the building in depth and obtain the point cloud.

- Preprocessing compilations for the creation of the 3D model where the steps of dense cloud, built mesh, built texture and tiled model are performed using the same Agisoft Metashape software.

- Editing the 3D model and obtaining a solid model of the building with the Meshmixer software. The trees around the building have been removed and the building has been cut to obtain a flat base.

- Preparation of the model for 3D printing with PrusaSlicer software. The model has been sliced to define each pass of the printer, as well as the internal structure of the model to make it lighter.

- 3D printing of the model with the Original Prusa i3 MK3S 3D printer controlled through the Pronterface software.

This is a summary of the 19 steps of the elaborated method. We have managed to obtain a 3D printing of the building to evaluate the accuracy of the devised method.

Concerning the second research question on how to estimate the thermal transmittance of building walls using thermal images, we have employed the method developed in (Bayomi et al., 2021). Using equation (*4*) given in section 3.5.3 we obtained an estimate of the U-value. The parameters needed to obtain the U-value were collected using a FLIR i7 hand-held thermal camera, which allowed us to collect the temperature of the inner surface of the wall, the temperature of the outer surface of the wall and the reflection temperature. We have obtained a U-value with a deviation of 11.60% over the reference value obtained from real-time monitoring. It should be noted that this method is very sensitive to the temperature of the inner surface of the wall, as it is a very relevant parameter in equation (*4*).

Finally, to answer the third research question about how do the U-values obtained from real monitoring using heat flow sensors, calculation method according to the standard ISO 9869, and estimations based on thermal imaging differ in terms of accuracy, speed, cost, and usability, we have elaborated Table 4-6 in section 4.4. The general conclusions drawn from the comparison are that the most accurate method is real-time monitoring, but it requires more time, costs more, and is more complex than other methods. Quite the opposite of the calculation according to the standards, which has very poor accuracy but requires the least in the other terms. Finally, the estimation from IRT is between the other two methods, which with a very short time we can achieve accuracy close to reality.

5.2 Findings and Recommendations

In this section, we explain the findings of this study together with important recommendations based on the experience gained. We will start by discussing the findings and recommendations of the developed methods of obtaining the thermal transmittance (U-value) of the walls of the analysed building, followed by the proposed

method of 3D printing with its findings and recommendations. We will end with our general recommendations useful for possible future work.

As the results of chapter 4 of the paper have shown, the most accurate method to obtain a thermal transmittance closer to reality is real-time monitoring using the gSKIN U-Value Kit. A value of 1.86 W/m^2·K has been obtained, which confirms the poor thermal insulation of the building walls. On the other hand, this method is the one that requires the longest calculation time of a minimum of 73 hours. At the same time, it also has a high equipment cost and it is easy to make mistakes during the installation of the monitoring as certain requirements must be met. We recommend placing the indoor and outdoor sensors at the same place on the wall, i.e. in front of each other but on either side of the wall. It is also advisable to place them on a shaded wall where they will not be exposed to direct sunlight, and that they will be sheltered in case it rains during the monitoring period.

Regarding the results obtained by the calculation according to the ISO 9869 standard, the calculated result of 0.46 W/m^2·K is far from the real value. This fact confirms that the insulation components of the wall, specifically the rock wool, are in very bad condition due to the many years since the construction of the building. It is possibly deteriorated and wet since the U-value obtained corresponds to insulation in perfect condition and with a very low thermal conductivity of 0.035 W/m·K. We have estimated the value of the real thermal conductivity obtaining a value of 0.285 W/m·K, as we have seen in section 4.2. The speed, cost and usability parameters of this method are very favourable, although they do not compensate in any way for the very low accuracy.

If we now look at the results of the U-value estimation using thermal imaging, we have obtained a value of 1.64 W/m^2·K. We can consider that this value is close to the real reference value as it presents a deviation of 11.60%. However, the equation used has to be taken with caution, since as we have explained above, this equation is very sensitive to the inner surface temperature of the wall since this parameter appears 3 times in equation (*4*). This method falls in between the other two in terms of accuracy, speed, cost and usability. However, it stands out above all in the speed of estimation, as it allows you to obtain the U-value in approximately 3 hours, much less than the real-time monitoring method. The main recommendation of this method is when obtaining surface temperatures through a thermal or infrared camera because if you take the thermal images with a high % of ambient humidity due to e.g. rain or fog, the temperature readings can vary a lot and highly alter the results. For this reason, we recommend paying special attention to the ambient conditions when capturing the thermal images.

A large part of this study has been to elaborate the methodology for obtaining a 3d printing or model of the building under analysis from the images captured with the drone. We can conclude that we have built a 19-step process in section 3.5.4 that has helped us to obtain 3D printing with good accuracy. The final 3D printing has a good higher definition on the roof and its contour. On the other hand, other more specific and smaller parts of the building, such as windows or hidden corners of the building, are less well defined. We have faced some problems such as the presence of a very large tree in a corner of the building that completely covered a façade and the irregularity of the base of the building, due to the unevenness of the terrain where it is located. In both cases, it was necessary to carefully cut the model. We would like to

highlight two recommendations on image capture, which is of great importance as it is the basis of the 3D model with the Agisoft software. The first is to try to avoid capturing images with reflections or shadows from the sun, so it is preferable to choose a cloudy day with uniform light. The other recommendation is to capture images from all angles and positions of the building, preferably perpendicular to the building façade.

To conclude, we have carried out an analysis of the thermal camera drone market and we would like to propose the two models that we think will be the most interesting for the year 2021:

- DJI Matrice 300 RKT with the thermal camera Zenmuse H20T.

- DJI MAVIC Enterprise Advanced (with built-in thermal camera).

These two drones have considerable dimensions and for this reason, it is necessary to have a UAB driving licence and to apply for permission from the territorial administration before each mission. Using these drones allows you to get a very good resolution of thermal images while allowing you to thermally analyse the entire building envelope, which was not possible in this study. The technical descriptions and the market prices of these two drones can be found in Annex 7 and Annex 8.

5.3 Strength and Limitations

This chapter is dedicated to discussing the strengths and limitations developed throughout this study.

The calculations and analyses carried out in this thesis follow strict standards, recognised and exposed in the literature. The use of a normative basis is a guarantee of seriousness and leads to results that can be easily reused for future research. The methods involved in the calculation or estimation of thermal transmittance are described transparently and in detail, thus ensuring that the work meets expectations. Furthermore, the results obtained throughout this thesis are provided in detail. These elements make this work a potential basis for future studies.

We have elaborated a methodology of how to build a 3D model of a building from images obtained by a drone through 19 very detailed steps, which facilitates the reproduction of the method. The exhaustive following of this methodology can serve as a basis for future research or practice. This methodology has allowed us to learn about different fields that we were unfamiliar with, such as drone driving, 3D modelling from images and 3D printing.

Calculations and estimations of the thermal transmittance of the building façade have been carried out which corroborate the hypothesis that the insulation material of the façades is in a high degree of degradation and causes very significant thermal losses. The types of anomalies of the facades have been detected using thermal images.

The first important limitation we had to face was the fact that we did not have a drone equipped with a thermal camera. For this reason, we could only analyse the building thermally from the ground with a handheld thermal camera with limited resolution.

Another limitation is that we have only been able to collect thermal transmittance data from one room in the building with contact to the outside, as the residence analysed is highly occupied and we had limited access. In addition, the limited time available for

data collection and analysis did not allow us to compare data from different parts of the building envelope.

5.4 Implications on practice and future work

In this work, we have carried out the estimation of thermal transmittance from thermal images. We have compared and evaluated this method with other ways of calculating the thermal transmittance of a wall supported by recognised standards. This estimation allows us to obtain a fairly good U-value close to reality in a short time interval and at a moderate cost. The importance of this method for the analysis of a building envelope should be emphasised, allowing the detection of anomalies in the façade and relevant heat losses in a short period of a few hours.

We have elaborated a detailed and very complete methodology to obtain 3D printing from the simple images collected by a drone. This comprehensive and simple methodology is intended to serve as a foundation for future users to build 3D models using image recognition.

This work is done as a basis for future research work in the SBD Lab. The next steps of this work would be to use a drone equipped with a thermal camera to capture information from the entire envelope of a building. These thermal images can be added to the 3D model of the building elaborated in this study to obtain a complete 3D thermal model. In this way, heat losses and anomalies can be easily detected in detail from the building envelope.

Another method to obtain the thermal transmittance of a building is to create a building energy model (BEM). Therefore, future work will consist of modelling the building in software such as DesignBuilder and Energy plus. In this way, it will be possible to compare the 3D thermal model of the building created from the thermal images of the drone with the BEM.

6 Conclusions

At the beginning of this study, the definition of the problem has been raised. In the region of Wallonia, there are many houses built in the 1960s after the Second World War. These houses have deteriorated envelopes and façades over the years and are energetically very deficient and have significant heat losses. This work aims to achieve a methodology for quick diagnosis of buildings envelopes in order to identify the elements that need future renovation.

The main objective of this work is to find a tool for the detection of anomalies in the envelope of a building using infrared thermography. The variable used is the thermal transmittance (U-value) of the walls of the building to evaluate the state of its. We have calculated the U-value using three ways such as real-time monitoring, calculation according to ISO 9869 standards and estimation from thermal images. Subsequently, a comparison of the three methods has been carried out in terms of accuracy, speed, cost and usability. Furthermore, during this work, a methodology has been elaborated to obtain a 3D impression model of the residence building of the University of Liege from the images captured by a drone. This work aims to evaluate the accuracy of this methodology to be a basis for future research on 3D building modelling from thermal images obtained with thermal drones.

The first research question posed is about how to achieve 3D printing from images obtained by a drone. To answer this question, we have elaborated a detailed methodology of 19 steps, where from 270 aerial images of the building, we have obtained a 3D printing of the building at a scale of 1:400 with a quite good accuracy as we have seen in chapter 4 Results. A brief summary of the main steps of this methodology is capturing the images with the UAB, image recognition and model creation with the Agisoft Metashape software, polishing and making the solid model with the Meshmixer software, preparing the model for 3D printing with the PrusaSlicer software and finally printing the 3D printing.

The second question asks how to estimate the thermal transmittance value (U-value) of a building envelope using thermal images. The estimation has been made from equation (*4*) of the paper where we have obtained a value of 1.64 W/m^2·K quite close to the real U-value with a deviation of 11.60%. The inputs used for the estimation and obtained from infrared images with a hand-held camera have been the interior and exterior surface temperatures of the building as well as the reflection temperature. Although the estimation obtained is quite good, we have found that this estimation has to be used with caution as it is very sensitive to the inner surface temperature of the wall.

The third and the last research question ask about how do the U-values obtained from real monitoring using heat flow sensors, calculation method according to the standard ISO 9869, and estimations based on thermal imaging differ in terms of accuracy, speed, cost, and usability. To answer this question we have prepared a comparison table of the three methods of obtaining the U-value in the four terms of analysis. The most accurate method is real-time monitoring, but it requires more time, costs more, and is more complex than other methods. Quite the opposite of the calculation according to the standards, which has very poor accuracy but requires the least in the

other terms. Finally, the estimation from IRT is between the other two methods, which with a very short time we can achieve accuracy close to reality.

The results obtained from the thermal transmittance have confirmed that the insulation materials of the walls of the building show a further degradation, as the U-value obtained from the real-time monitoring is very unfavourable with a value of 1.86 W/m^2·K. Moreover, through the thermal images obtained from the building envelope, the presence of three important anomalies such as thermal bridging, insulation failure and degradation of the façade material has been found. For this reason, we can conclude that it would be interesting to consider remodelling the building envelope to improve the severe heat losses.

Finally, this work is intended to serve as a knowledge base for future research work, such as the 3D thermal modelling of a building from thermal images obtained with a thermal drone, which could be very interesting to evaluate the globality of the building envelope. It would also be interesting to work on and improve the estimation of the U-value from thermal images, as this system allows to detection of important heat losses by obtaining a value of the thermal transmittance of parts of the building in a reduced time and effort.

7 References

Agisoft Metashape User Manual: Professional Edition, Version 1.8 (pp. 1–9). (2022). Agisoft LLC. https://www.agisoft.com/downloads/user-manuals/

Agisoft PhotoScan Professional 1.4.3. (2022). Agisoft. https://www.agisoft.com/

ASTM E1862-97. (1997). Standard Test Methods for Measuring and Compensating for Refliected Temperature Using Infrared Imaging Radiometers. *American National Standard*.

Attia, S., Mustafa, A., Giry, N., Popineau, M., Cuchet, M., & Gulirmak, N. (2021). Developing two benchmark models for post-world war II residential buildings. *Energy and Buildings*, *244*, 111052.

Bayomi, N., Nagpal, S., Rakha, T., & Fernandez, J. E. (2021). Building envelope modeling calibration using aerial thermography. *Energy and Buildings*, *233*, 110648.

FLIR Thermal Studio. (2021). Teledyne FLIR LLC. https://www.flir.com/products/flir-thermal-studio-suite/

Fox, M., Coley, D., Goodhew, S., & De Wilde, P. (2014). Thermography methodologies for detecting energy related building defects. *Renew Sustain Energy Rev*, *40*, 296–310.

Francesco, A., Baldinelli, G., & Francesco, B. (2011). A quantitative methodology to evaluate thermal bridges in buildings. *Appl Energy*.

International Energy Agency (IEA). (2014). *Technology Roadmap "Energy Efficient Building Envelopes."*

IPCC. (2014). *Climate Change 2014: Synthesis Report. Contribution of Working Groups I, II and III to the Fifth Assessment Report of the Intergovernmental Panel on Climate Change* (IPCC; p. 151). [Core Writing Team, R.K. Pachauri and L.A. Meyer (eds.)].

ISO 6946. (2017). Building components and building elements—Thermal resistance and thermal transmittance—Calculation methods. *Irish Standard*.

ISO 9869-1. (2014). Thermal insulation—Building elements—Insitu measurement of thermal resistance and thermal transmittance Part 1: Heat flow meter method. *BSI*.

Kylili, A., Fokaides, P.A., Christou, P., & Kalogirou, S.A. (2014). Infrared thermography (IRT) applications for building diagnostics: A review. *Appl Energy*, *134*(531–49).

Madding, R. (2008). Finding R-values of stud-frame constructed houses with IR thermography. *Proc. InfraMarion, Reno, USA*.

Maharani, M., Charieninna, A., & Nugroho, H. (2020). Identification of photo number effect for 3D modeling in Agisoft software. *IOP Conference Series: Earth and Environmental Science*, *500*(1), 012073. https://doi.org/10.1088/1755-1315/500/1/012073

Mauriello ML, Norooz L, Froehlich JE. (2015). Understanding the role of thermography in energy auditing: Current practices and the potential for automated solutions. *Conf Hum Factors Comput Syst*.

Meshmixer 3.5. (2021). Autodesk Inc.
https://www.autodesk.com/research/projects/meshmixer

O'Grady, M., Lechowska, A.A., & Harte, A.M. (2017). Quantification of heat losses through building envelope thermal bridges influenced by wind velocity using the outdoor infrared thermography technique. *Energy*, *208*(1038–52).

Pearson, C. (2011). Thermal Imaging of Building Fabric. *BSRIA*.

Pronterface. (2021). Printrun. https://www.pronterface.com/

PrusaSlicer 2.3.3. (2021). Prusa Research.
    https://www.prusa3d.com/page/prusaslicer_424/

Rakha, T. & Gorodetsky, A. (2018). Review of Unmanned Aerial System (UAS)
    applications in the built environment: Towards automated building inspection
    procedures using drones. *Autom Constr*, *93*(252–64).

Rakha, T., Liberty, A., Gorodetsky, A., Kakillioglu, B., & Velipasalar, S. (2018). Heat
    Mapping Drones: An Autonomous Computer-Vision-Based Procedure for
    Building Envelope Inspection Using Unmanned Aerial Systems (UAS).
    Technology|Architecture + Design, *2*, 30–44.
     https://doi.org/10.1080/24751448.2018.1420963

Rakha, T., Masri, Y. E., Chen, K., & Wilde, P. D. (2021). *3D Drone-based Time-lapse
    Thermography: A Case Study of Roof Vulnerability Characterization using
    Photogrammetry and Performance Simulation Implications*. 8.

Schwoegler, M. (2006). Infrared Thermography Basics. *Stockholm*.

Tanner, C., Lehmann, B., & Frank KGW, T., F. (2011). A proposal for standardized
    thermal images. *Bauphysik*, *33*, 345–356.

Thumann, P.E., C.E.M. A, Younger, C.E.M. WJ. (2017). *Handbook of Energy Audits*.

Annexes

Annex 1: gSKIN® KIT U-Value Kit data-sheet

gSKIN® KIT U-Value Kit

FEATURES

- Calibrated Plug-and-Play solution
- Measurement of U-Value (W/(m²K)), heat flux (W/m²), and 2 temperatures (°C)
- Compatible with standards ISO 9869 and ASTM C1046 / ASTM C1155
- Stores up to 2 million data points
- Battery lifetime >1 month
- High sensitivity thermal detectors
- Read-out software included
- Compact design
- USB interface

gSKIN®-XO 67 7C   DLOG-4231   Transport box

Product Name	gSKIN® KIT-2615C
Article Number	A-163479
gSKIN® KIT includes [a]	Sensor: gSKIN®-XO 67 7C (30mm x 30mm) Logger: DLOG-4231 incl. 2 temperature sensors Software Mounting Tape
Heat Flux Range Min / Max [W/m²]	±200[d]
Heat Flux Resolution [W/m²]	<0.22
Min. Sensor Sensitivity [a] (S) [μV/(W/m²)]	7
Temperature Sensor Accuracy [°C]	±0.5 (-10...+65 °C) ±2.0 (-55...+125 °C)
Logger Dimensions (l x w x h) [mm x mm x mm]	52 x 20 x 15
Measurement Frequency	1/sec to 1/h
Bit Resolution [bits]	12
Data Storage Capacity [# measurements]	>2'000'000
Battery Lifetime [c] [days]	>30 (rechargeable)
Computer Interface	USB
Software	Installation-SW sent by email / via download link
Operating System	Windows 2000 / XP / Vista / 7 / 8
Operation Modes	Live display / Data logger
Operating Temperature Range Min/Max [°C]	-40 / 100 (-20 / 65 for Logger)
Calibration Temperature Range Min/Max [°C]	-30 / 70
Calibration Accuracy [b] [±%]	3
Temperature Sensor 1 / 2 Cable Length [m]	5.0 / 1.0
Heat Flux Sensor / Logger Cable Length [m]	1.0 / 0.5 (with connectors)

[a] For more details consult the datasheets of the individual products.
[b] Sensor calibration data already loaded onto logger for simple and fast plug-and-play measurements.
[c] At lowest measurement frequency (2/d).
[d] Heat Flux Range up to +/- 400 [W/m²] available on request

Datasheet V3.6, © Copyright greenTEG AG, 2014 All Rights Reserved
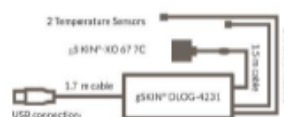
2 Temperature Sensors
gSKIN®-XO 67 7C
1.7 m cable
gSKIN® DLOG-4231
USB connection

Annex 2: Plan of the first floor of B13 building

Annex 3: FLIR i7 data-sheet

FLIR i-Series

The Most Affordable Point-and-Shoot Infrared Cameras Just Got Better

More powerful than ever, i-Series improves your options with a strong line-up of fresh choices to fit the level of detail your application requires. Featuring the new i7, now with 36% higher thermal resolution than before and a wider field of view to help you image more clearly, scan more quickly, and store an entire scene in one complete picture.

Three Best-in-Class Imagers – FLIR i3 – 3,600 pixels; FLIR i5 – 10,000 pixels; FLIR i7 – 19,600 pixels

Accuracy – Temperature accuracy calibrated within ±2°C or 2% of reading to meet the standard you can always trust FLIR to deliver

Compact Design – Light at 13 ounces (365g) for easy one-handed operation yet tough enough to stow with the rest of your tools

Optimized Temperature Range – From −4 to 482°F (−20 to 250°C) for electrical, industrial and building applications

Radiometric Images – Stores up to 5,000 JPEG image files with all temperature measurements right in the camera ready to download for further analysis and custom reports

Focus Free Lens – For convenient viewing

High Resolution Color LCD – 2.8" (71mm)

Measurement Modes – All models - Spot (center); FLIR i7 also features Area (Min/Max)

Thumbnail Image Gallery – Allows quick search of stored images

Li-Ion Rechargable Battery – provides >5 hours continuous use, is replaceable, and features an in-camera charging system

Includes – 2G miniSD Card with adaptors, Li-Ion rechargeable battery with 100-240V AC adaptor/charger with EU, UK, US and Australian plugs, mini USB cable, FLIR Tools reporting software, built-in manual lens shutter, and hard case

Find Hot Spots Fast!

Focus-free Lens for Point-and-Shoot Simplicity
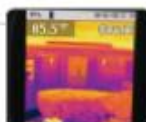
Excellent 2.8" Color LCD Shows the Whole Scene

Removable SD Card and USB Output for Fast Image Downloads

Includes Hard Case

FLIR

Why Thermal Imaging?
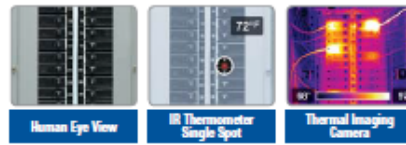
While spot IR thermometers offer only a single temperature readout, thermal imaging cameras give you the whole picture, equal up to 19,600 spots (FLIR i7)! Thermal imaging is the most effective method for finding problems or potential problems in a variety of applications across many fields. If you are new to Thermography and need a general purpose infrared camera for troubleshooting, the FLIR i3, FLIR i5 or FLIR i7 is perfect for you!

Imaging Specifications

FEATURES	FLIR i3	FLIR i5	FLIR i7
Thermal sensitivity (N.E.T.D)	<0.15°C at 25°C	<0.1°C at 25°C	<0.1°C at 25°C
Field of view/min focus distance	12.5° x 12.5°/0.6m (2 ft.)	21° x 21°/0.6m (2 ft.)	29° x 29°/0.6m (2 ft.)
Detector Type - Focal plane array (FPA) uncooled microbolometer	60 x 60 pixels	100 x 100 pixels	140 x 140 pixels
Measurement modes	Spot	Spot	Spot, Area (Max/Min)
Isotherm	—	—	Above/Below
COMMON FEATURES			
Temperature range	-4°F to 482°F (-20°C to 250°C)		
Image Storage	5000 Images (microSD card memory)		
Emissivity	Emissivity Table; 0.1 to 1.0 adjustable		
Frame Rate	9Hz		
Focus	Focus free		
Spectral range	7.5 to 13µm		
Display	Built-in 2.8" color LCD		
Image modes	Thermal - Palettes (Iron, Rainbow, and Black/White)		
Set-up controls	Date/time, °C/°F, 21 languages		
Battery Type/operating time	Li-Ion/ >5 hours, Display shows battery status		
Charging system	In camera, AC adapter; 3 hours to 90% capacity		
Shock/Vibration/Drop / Encapsulation; Safety	25G, IEC 60068-2-29 / 2G, IEC 60068-2-6 / Drop-proof 2m (6.6ft) IP43; UL, CSA, CE, PSE and CCC		
Dimensions/Weight	8.8x3.1x3.4" (223x79x85mm)/<12.9oz. (365g), including battery		
Warranty	2/5/10 (Camera-2 years, Battery-5 years, Detector-10 years)		

Ordering Information

60101-0101.................. FLIR i3 Compact Thermal Imaging InfraRed Camera (60x60)
60101-0101-NIST.......... FLIR i3 with Certificate Traceable to NIST

60101-0201 .... FLIR i5 Compact Thermal Imaging InfraRed Camera (100x100)
60101-0201-NIST.......... FLIR i5 with Certificate Traceable to NIST

60101-0301 .... FLIR i7 Compact Thermal Imaging InfraRed Camera (140x140)
60101-0301-NIST.......... FLIR i7 with Certificate Traceable to NIST

ACCESSORIES
T911085........................ Pouch for FLIR ix-series
T911093........................ Tool Belt
T911025........................ Car Charger
T910711 .... Power supply/charger with EU, UK, US and AU plugs
T197410 .... Rechargeable Li-Ion Battery
T197619 .... Hard Transport Case

10-Year Detector
Protection
5-Year Battery
2-Year Parts & Labor

FLIR

Annex 4: DJI Mini 2 data-sheet
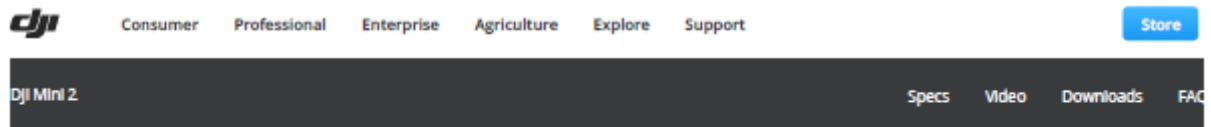
Specs

Aircraft

Takeoff Weight [1]	< 249 g
Dimensions	Folded: 138×81×58 mm (L×W×H) Unfolded: 159×203×56 mm (L×W×H) Unfolded (with propellers): 245×289×56 mm (L×W×H)
Diagonal Distance	213 mm
Max Ascent Speed	5 m/s (S Mode) 3 m/s (N Mode) 2 m/s (C Mode)
Max Descent Speed	3.5 m/s (S Mode) 3 m/s (N Mode) 1.5 m/s (C Mode)
Max Speed (near sea level, no wind)	16 m/s (S Mode) 10 m/s (N Mode) 6 m/s (C Mode)
Max Service Ceiling Above Sea Level	4000 m
Max Flight Time	31 mins (measured while flying at 4.7 m/s in windless conditions)
Max Wind Speed Resistance	8.5-10.5 m/s (Scale 5)
Max Tilt Angle	40° (S Mode) 25° (N Mode)* 25° (C Mode)* * Up to 40° under strong winds
Max Angular Velocity (by default)*	130°/s (S Mode) 60°/s (N Mode) 30°/s (C Mode) * Can be adjusted to 250°/s with the DJI Fly app
Operating Temperature	0° to 40°C (32° to 104°F)
Operating Frequency [2]	2.400-2.4835 GHz, 5.725-5.850 GHz
Transmitter Power (EIRP)	2.400-2.4835 GHz FCC ≤ 26 dBm CE ≤ 20 dBm SRRC ≤ 20 dBm 5.725-5.850 GHz FCC ≤ 26 dBm CE ≤ 14 dBm SRRC ≤ 26 dBm

Global Navigation Satellite System (GNSS)	GPS+GLONASS+GALILEO
Hovering Accuracy Range	Vertical: ±0.1 m (with Vision Positioning), ±0.5 m (with GPS Positioning) Horizontal: ±0.3 m (with Vision Positioning), ±1.5 m (with GPS Positioning)

Gimbal

Mechanical Range	Tilt: -110° to 35° Roll: -35° to 35° Pan: -20° to 20°
Controllable Range	Tilt: -90° to 0° (default setting) -90° to +20° (extended)
Stabilization	3-axis (tilt, roll, pan)
Max Control Speed (tilt)	100°/s
Angular Vibration Range	±0.01°

Sensing System

Downward	Hovering Range: 0.5-10 m
Operating Environment	Non-reflective, discernable surfaces Diffuse reflectivity (> 20%, such as cement pavement) Adequate lighting (lux > 15, Normal exposure environment of indoor fluorescent lamp)

Camera

Sensor	1/2.3" CMOS Effective Pixels: 12 MP
Lens	FOV: 83° 35 mm format equivalent: 24 mm Aperture: f/2.8 Focus range: 1 m to ∞
ISO	Video: 100-3200 (Auto) 100-3200 (Manual) Photos: 100-3200 (Auto) 100-3200 (Manual)
Shutter Speed	Electronic Shutter: 4-1/8000 s
Max Image Size	4:3: 4000×3000 16:9: 4000×2250
Still Photography Modes	Single Shot Interval: JPEG: 2/3/5/7/10/15/20/30/60 s JPEG+RAW: 5/7/10/15/20/30/60 s Auto Exposure Bracketing (AEB): 3 bracketed frames at 2/3 EV Bias Panorama: Sphere, 180°, and Wide-angle
Video Resolution	4K: 3840×2160 @ 24/25/30fps 2.7K: 2720×1530 @ 24/25/30/48/50/60fps FHD: 1920×1080 @ 24/25/30/48/50/60fps

Max Video Bitrate	100 Mbps
Zoom Range	4K: 2x 2.7K: 3x FHD: 4x
QuickShot Modes	Dronie, Helix, Rocket, Circle, Boomerang
Supported File Formats	FAT32 (≤ 32 GB) exFAT (> 32 GB)
Photo Formats	JPEG/DNG (RAW)
Video Formats	MP4 (H.264/MPEG-4 AVC)

Remote Controller & Video Transmission

Operating Frequency	2.400-2.4835 GHz, 5.725-5.850 GHz
Max Transmission Distance (unobstructed, free of interference) [3]	10 km (FCC) 6 km (CE) 6 km (SRRC) 6 km (MIC)
Signal Transmission Ranges (FCC) [4]	Strong Interference (urban landscape, limited line of sight, many competing signals): Approx. 3 km Medium Interference (suburban landscape, open line of sight, some competing signals): Approx. 6 km Low Interference (open landscape abundant line of sight, few competing signals): Approx. 10 km
Operating Temperature	-10° to 40° C (14° to 104° F)
Transmission Power (EIRP)	2.400-2.4835 GHz FCC ≤ 26 dBm CE ≤ 20 dBm SRRC ≤ 20 dBm MIC ≤ 20 dBm 5.725-5.850 GHz FCC ≤ 26 dBm CE ≤ 14 dBm SRRC ≤ 26 dBm
Battery Capacity	5200 mAh
Voltage	1200 mA 3.6 V (Android) 700 mA 3.6 V (iOS)
Supported Mobile Device Size	180×86×10 mm (Height×Width×Thickness)
Supported USB Port Types	LightningMicro USB (Type-B) USB-C
Video Transmission System	When used with different aircraft hardware configurations, both remote controllers will automatically se corresponding firmware version for updating and support the following transmission technologies enab hardware performance of the linked aircraft models: a. DJI Mini 2/ DJI Mavic Air 2: O2 b. DJI Air 2S: O3 c. DJI Mavic 3: O3+
Live View Quality	Remote Controller: 720p/30fps
Max Bitrate	8 Mbps

Latency (depending on environmental conditions and mobile device)	About 200 ms

Charger

Input	100-240 V, 50/60 Hz, 0.5 A
Output	12V 1.5 A / 9V 2A / 5V 3A
Rated Power	18 W

Intelligent Flight Battery

Battery Capacity	2250 mAh
Voltage	7.7 V
Charging Voltage Limit	8.8 V
Battery Type	LiPo 2S
Energy	17.32 Wh
Weight	86.2 g
Charging Temperature	5° to 40°C (41° to 104°F)
Max Charging Power	29 W

App

Name	DJI Fly
Required Operating System	iOS v10.0 or laterAndroid v6.0 or later

Supported SD Cards

Supported SD Cards	UHS-I Speed Class 3 or above is required. A list of recommended microSD cards can be found below.
Recommended microSD Cards	16 GB: SanDisk Extreme 32 GB: Samsung Pro Endurance, Samsung Evo Plus, SanDisk Industrial, SanDisk Extreme V30 A1, SanDisk A2, SanDisk Extreme Pro V30 A1, SanDisk Extreme Pro V30 A2, Lexar 633x, Lexar 667x 64 GB: Samsung Pro Endurance, Samsung Evo Plus, SanDisk Extreme V30 A2, Lexar 633x, Lexar 667x, Lexar High Endurance, Toshiba EXCERIA M303 V30 A1, Netac Pro V30 A1 128 GB: Samsung Evo Plus, SanDisk Extreme V30 A2, SanDisk Extreme Plus V30 A1, SanDisk Extreme Plus 633x, Lexar 667x, Lexar 1000x, Lexar High Endurance, Toshiba EXCERIA M303 V30 A1, Netac Pro V30 A1 256 GB: SanDisk Extreme V30 A2

Footnotes

Footnotes	1. The standard weight of the aircraft (including battery, propellers, and a microSD card) is 242 grams. Ac weight may vary. Registration is not required in some countries and regions. Check local rules and regula use. These specifications have been determined through tests conducted with the latest firmware. Firmw can enhance performance, so updating to the latest firmware is highly recommended.

2. Due to local policy and regulation restrictions, the 5.8 GHz frequency band is currently banned in certa
including but not limited to Japan, Russia, Israel, Ukraine, and Kazakhstan. Please use the 2.4 GHz freque
when operating in these locations. Always check local rules and regulations before use, as they may char
3. Maximum flight range specification is a proxy for radio link strength and resilience, not aircraft battery
only refers to the maximum, one-way flight distance. Data was measured in an open environment withou
interference. Please pay attention to the return prompt on the DJI Fly app during actual flight. Refer to the
applicable standard in different countries and regions:
FCC: United States, Australia, Canada, Hong Kong, Taiwan, Chile, Colombia, Puerto Rico, and other region
SRRC: Mainland China;
CE: UK, Russia, France, Germany, Portugal, Spain, Switzerland, Macau, New Zealand, UAE, and other regio
MIC: Japan.
4. Data is tested under different standards in open areas free of interference. It only refers to the maximu
flight distance without considering Return to Home. Please pay attention to RTH prompts in the DJI Fly ap
actual flight.

Annex 5: Original Prusa i3 MK3S data-sheet

Original Prusa i3 MK3S+ 3D printer

★★★★☆ 4 reviews

The Original Prusa i3 MK3S+ is the latest version of our award-winning 3D printers. We have upgraded the MK3S with a brand **new SuperPINDA** probe for improved first layer calibration, added high-quality **Misumi bearings** and made various useful **design tweaks**.

The printer also includes a free 1kg filament spool of Silver PLA!

Alternatively, you can try the full "Prusa Experience" with the printer kit, which you will assemble by yourself (it takes around 8 hours), and learn more about how the printer work.

Original Prusa i3 MK3S+ kit

Leadtime 5–6 weeks

€769
€635.54 without VAT

Detail

Technical Parameters

Build Volume	25×21×21 cm (9.84"×8.3"×8.3")
Layer height	0.05 - 0.35 mm
Nozzle	0.4mm default, wide range of other diameters/nozzles supported
Filament diameter	1.75 mm
Supported materials	Wide range of thermoplastics, including PLA, PETG, ASA, ABS, PC (Polycarbonate), CPE, PVA/BVOH, PVB, HIPS, PP (Polypropylene), Flex, nGen, Nylon, Carbon filled, Woodfill and other filled materials.
Max travel speed	200+ mm/s
Max nozzle temperature	300 °C / 572 °F
Max heatbed temperature	120 °C / 248 °F
Extruder	Direct Drive, Bondtech gears, E3D V6 hotend
Print surface	Removable magnetic steel sheets(*) with different surface finishes, heatbed with cold corners compensation
Printer dimensions (without spool)	7 kg, 50×55×40 cm; 19.6×21.6×15.7 in (X×Y×Z)
Power consumption	PLA settings: 80W / ABS settings: 120W

* Consumable parts, such as PEI sheets (smooth, textured, etc.) are not covered by warranty as the coatings are designed to diminish over time unless failure has occurred due to a defect in materials or workmanship. Cosmetic damage, including but not limited to scratches, dents, cracks, or other cosmetic damage is also not covered by the warranty. Only defective sheets on arrival are covered by warranty.

Annex 6: Real-time monitoring greenTEG report

![greenTEG logo]

Measurement result:

Logger data:

Serial No:	327434		
Type:	U-value measurement kit	Inside temp. (T1):	18.9 °C
Sensitivity:	11.9 uV/(W/m²)	Outside temp. (T2):	3.5 °C
Config.:	CB125BA	Measurement time (t):	118.73 h

U-value analysis using average method (Section 7.1, ISO 9869-1:2014):

Analysis start time:	2021-11-25 17:42:44	U-value w/o last 24h (U24):	1.88 W/(m²K)
Analysis end time:	2021-11-28 17:42:44	U-value first 2/3 (U2/3):	1.88 W/(m²K)
Analysis period:	72 h	U-value last 2/3 (U2/3):	1.84 W/(m²K)
		dU24:	-1.1 %
U-value:	1.86 W/(m²K)	dU2/3:	2.1 %
		dR24:	1.6 %
		dR2/3:	-3.0 %

Measurement data fulfils requirements of ISO 9869-1:2014 section 7.1.

Uncertainties due to improper installation or environmental influences must be estimated by user (see section 6.1).

Additional comments:

Measurement overview over t=118.73 h
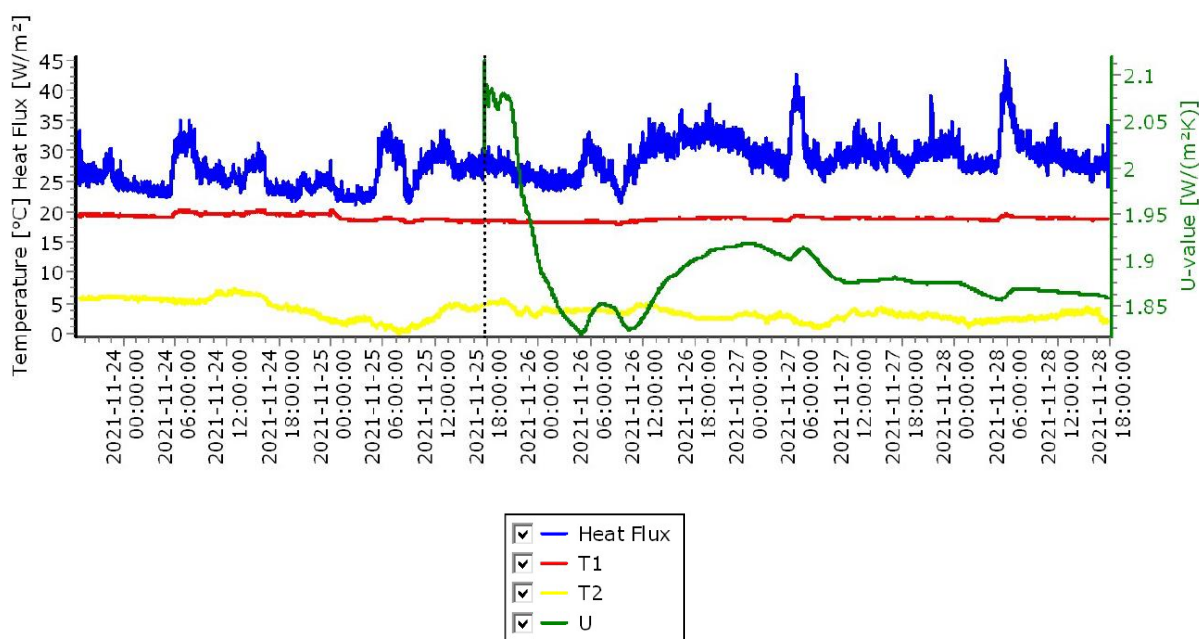
Annex 7: DJI Matrice 300 RKT + Zenmuse H20T

In the Box

Aircraft Body × 1	**DJI Smart Controller Enterprise** × 1	**USB Charger** × 1	**USB-C Cable** × 1	**TB60 Intelligent Flight Battery** × 2	**WB37 Intelligent Battery** × 1
2110 Propeller (CW) (pair) × 1	**2110 Propeller (CCW) (pair)** × 1	**Landing Gear** × 2	**Spare Stick Cover (pair)** × 1	**Spare Propeller Holder** × 2	**Spare Gimbal Damper** × 4
USB Cable (with Double A Ports) × 1	**Vision System Calibration Plate** × 1	**Carrying Case** × 1	**Smart Controller Lanyard** × 1	**Rubber Port Cover (Set)** × 1	**Screws and Tools** × 1
BS60 Intelligent Battery Station × 1					

Expected delivery date: 25/01/2022

26 300 € **Add to Cart**

Annex 8: DJI Mavic 2 Enterprise Advanced

DJI STORE   Camera Drones   Handheld   Education & Industry   Services

Mavic 2 Enterprise Advanced

6 400 €

- Max flight time: 31 min
- 10 km HD Video Transmission
- Centimeter-level Positioning with RTK
- 32× Digital Zoom
- Six-way obstacle avoidance

Overview ›

Warranty Notice

In the event of any paid repair due to non workmanship or material damage， an unlimited number of repair services can be offered within one year after the product is activated, with a free repair coverage equivalent to the product's value. For details on the warranty periods of individual components, please visit DJI's after-sales policies page.

In the Box

Aircraft
× 1

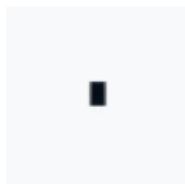DJI Smart Controller
× 1

Battery Charger
× 1

Power Cable
× 1

Propeller (pair)
× 3

Spare Control Stick (pair)
× 1

Communication Cable-USB 3.0 Type-C
× 1

24W USB Charger
× 1

Extended port cover
× 1

Speaker
× 1

Spotlight
× 1

Beacon
× 1

Protector Case
× 1

Ship within 1 business day, expected arrive date: 14/01/2022

6 400 €   Add to Cart